ESCOLA
SUPERIOR
DE SAÚDE
POLITÉCNICO
DO PORTO

P.PORTO

M

MESTRADO
BIOQUÍMICA EM SAÚDE

Food polyphenols interaction with bitter taste receptors

Maria Leonor Pestana Gonçalves

09/**2020**

P.PORTO

ESCOLA SUPERIOR DE SAÚDE

INSTITUTO DE INVESTIGAÇÃO E INOVAÇÃO EM SAÚDE
UNIVERSIDADE DO PORTO

U.PORTO
FACULDADE DE CIÊNCIAS
UNIVERSIDADE DO PORTO

Food polyphenols interaction with bitter taste receptors

Autor

Maria Leonor Pestana Gonçalves

Orientadores

Postdoctoral researcher, Susana Soares, FCUP | UP

PhD, Ricardo Ferraz, ESS | IPP

Co-orientador

PhD, Frederico Silva, IBMC | i3S

Dissertação apresentada para cumprimento dos requisitos necessários à obtenção do grau mestre em **Bioquímica em Saúde** – Ramo em **Bioquímica Clínica e Metabólica** pela Escola Superior de Saúde do Instituto Politécnico do Porto.

Financial support

This thesis was partially supported by the Project "BITTAST*y*" Ref. UIDB/50006/2020 at LAQV – Laboratório Associado para a Química Verde.

Agradecimentos

Este trabalho é dedicado a todos os que contribuíram para que esta dissertação fosse realizada. A todos vocês, muito obrigada.

Aos meus orientadores, Investigadora Pós-Doutorada Susana Soares, Doutor Frederico Silva e Professor Doutor Ricardo Ferraz quero expressar o meu muito obrigada por todo o apoio, disponibilidade, partilha do saber e as valiosas contribuições para o trabalho.

À Doutora Fátima Fonseca, um muito obrigada tanto pelos conhecimentos transmitidos, como pelo apoio e disponibilidade durante a realização do trabalho laboratorial.

Ao grupo *Cell Culture and Genotyping* (CCGen) do Instituto de Investigação e Inovação em Saúde (i3S), agradeço a ajuda, prontidão e simpatia que sempre demonstraram.

A toda a direção e professores do curso de mestrado de Bioquímica em Saúde, obrigada por me ter sido permitido o ingresso neste mestrado e por todo o conhecimento adquirido ao longo deste.

Ao Instituto de Investigação e Inovação em Saúde (i3S) e ao departamento de Química da Faculdade de Ciências da Universidade do Porto, agradeço a oportunidade de desenvolver este projeto.

A todos os meus amigos, muito obrigada pelo companheirismo, força e apoio.

Por último, agradeço aos meus pais, irmã e restante família, por todo o incentivo e apoio incondicional recebido ao longo destes anos.

Abstract

Polyphenols are widespread in plant-based foodstuffs contributing directly to their taste properties (astringency and bitter taste). Bitterness is perceived by activation of bitter taste receptors (TAS2Rs). Some polyphenols have been already identified as agonists for TAS2R5, TAS2R7 and TAS2R39. The aim of this study was to express and isolate TAS2R5, TAS2R7 and TAS2R39 on *S. cerevisiae* for further structure-activation studies. For this purpose, these TAS2Rs were expressed using a GFP-fusion yeast system. The transformants and the induction culture conditions (time, temperature, and addition of a chemical chaperone) were screened by whole-cell GFP fluorescence, immunoblotting and fluorescence microscopy. An increase of expression of TAS2Rs was observed when were induced with 2% of galactose at 20°C (TAS2R5), 26°C (TAS2R7), and with 2.5% of DMSO at 26°C (TAS2R39) for 22 hours. Isolation of TAS2R has been proven difficult due to cell lysis inefficiency and protein degradation. This study allowed to get insights on the best protein expression conditions for these TAS2Rs. The future work is focused on improving the isolation of these membrane proteins and finding alternative approaches. Ongoing work is developing two approaches based on a baculovirus expression vector system and on expression on an engineered GPCR-based signalling strain *S. cerevisiae*.

Keywords: Polyphenols; bitterness; bitter taste receptors; protein expression; activation screening.

Resumo

Os polifenóis existem em alimentos de origem vegetal, e contribuem diretamente para as propriedades organoléticas dos alimentos (adstringência ou sabor amargo). A perceção do gosto amargo ocorre pela ativação de recetores do sabor amargo (TAS2Rs). Alguns polifenóis já foram identificados como agonistas dos TAS2R5, TAS2R7 e TAS2R39. O objetivo desta dissertação foi expressar e isolar estes TAS2Rs para aprofundar a relação estrutura-atividade. Estes TAS2Rs foram expressos em *S. cerevisiae* através de um sistema de fusão com GFP. Os transformantes e as condições de cultura de indução (tempo, temperatura e adição de chaperonas químicas) ótimas foram estudadas através de "whole-cell fluorescence", "*immunoblotting*" e microscopia de fluorescência. Foi observado um aumento da expressão destes TAS2Rs quando estes foram induzidos com 2% galactose a 20°C (TAS2R5), 26°C (TAS2R7) e com 2.5% DMSO a 26°C (TAS2R39) durante 22 horas. O isolamento dos TAS2Rs demonstrou-se difícil, devido à falta de eficiência da lise celular e da inibição da degradação proteica. Este estudo permitiu averiguar algumas condições de expressão dos três TAS2Rs. Este trabalho tem como perspetivas futuras melhorar a expressão e isolamento destes TAS2Rs e procurar abordagens alternativas. Estão em curso métodos alternativos baseados noutro sistema de expressão (em Baculovírus) e baseados na expressão numa estirpe *S. cerevisiae* geneticamente modificada com sistema de sinalização de GPCR.

Palavras-chave: Polifenóis; sabor amargo; Recetores do sabor amargo; Expressão proteica; Screening da ativação.

Table of Contents

List of figures

List of tables

Abbreviations

AcMNPV	*Autographa californica* Multiple Nuclear Polyhedrosis Virus
BEVS	Baculovirus Expression Vector System
cDNA	complementary DNA
CHS	Cholesteryl hemisuccinate
DDM	*n*-Dodecyl-β-D-Maltopyranoside
DMSO	Dimethyl sulfoxide
EC_{50}	Half-Maximal Effective Concentrations
ECG	Epicatechin-3-*O*-gallate
EDTA	Ethylenediaminetertraacetic acid
EGCG	Epigallocatechin-3-*O*-gallate
Fwd	Forward
FLIRP	Fluorescence Imaging Plate Reader
FSEC	Fluorescence size-exclusion chromatography
GFP	Green fluorescent protein
GPCRs	G protein-coupled receptors
hpi	Hours post-infection
TAS2Rs	*human* Taste 2 Receptors
IMAC	Immobilized Metal-Ion Affinity Chromatography
PC	Phenolic compound(s)
PCR	Polymerase chain reaction
PGG	Pentagalloylglucose
PRPs	Proline rich salivary proteins
PVDF	Polyvinylidene difluoride
Rev	Reverse
SDS-PAGE	Sodium dodecyl sulphate – polyacrylamide gel electrophoresis
SNPs	Single-nucleotide polymorphisms
TAE	Tris-base Acetic acid and EDTA
TAS	Taste receptors
TMPs	Transmembrane proteins
TRCs	Taste Receptor Cells
URA	Uracil
WCF	Whole-cell fluorescence
yEGFP	Yeast enhanced green fluorescent protein
YFP	Yellow fluorescent protein
YPD	Yeast Peptone Dextrose
YSB	Yeast Suspension Buffer

1. Introduction

1.1. Bitter taste in relation to food polyphenols

Bitter taste usually receives consumers disapproval. However, it can also be appreciated, if only it is moderate, in products like coffee, beer, red wine, and dark chocolate [1, 2]. Bitter compounds are typically derived from plants (*e.g.*, caffeine in coffee, hop bitter acids in beer, naringin and naringenin in *Citrus* fruits, sinigrin in broccoli and brussels sprouts [3–7]). Nevertheless, they can also appear in products from animal origin (*e.g.*, bitter peptides in cheese [8]), food processing (*e.g.*, the Maillard reaction products – among which intensely bitter tastants such as quinizolate and homoquinizolate, among others [9]) and upon storage (*e.g.*, lipids oxidation [10]). In plants, the biological function of bitter compounds is to protect them from predators and pathogens, particularly toxins (*e.g.*, strychnine) which are often bitter [1, 11]. Thus, it has been presumed that the ability to perceive bitter compounds and its aversion has long been crucial to survival. Several natural bitter compounds have been also associated with putative health effects. In fact, polyphenols, which are a family of compounds widespread in plant-based foodstuffs with well-known healthy properties, contribute directly to their taste properties (*e.g.*, astringent sensation and bitter taste). Therefore, an unbiased recognition and knowledge on how and which polyphenols are bitter and/or astringent is necessary for a focused modulation of these sensory properties [1].

Bitter taste is mediated by a group of bitter taste receptor proteins that reside on the surface of taste cells within the taste buds of the tongue. These proteins are seven transmembrane domain, G protein coupled receptors, encoded by members of the TASTE 2 Receptors (TAS2R) gene family. The human genome contains 25 apparently functional TAS2R genes [1]. The major goals of chemosensory science are to functionally characterize these receptors and identify their ligands. However, this task has proven difficult, and the ligand that binds to each receptor and initiates bitter taste perception is known in only a few cases. Polyphenols such as epicatechin, procyanidins, pentagalloylglucose, punicalagin, malvidin-3-glucoside, have been already identified as agonists for some TAS2Rs, namely, TAS2R5, TAS2R7 and TAS2R39 [12, 13].

In this thesis, the main goal is to better understand the activation of TAS2Rs and by polyphenols. To achieve this goal, TAS2Rs will be expressed in different heterologous systems, such as yeast *Saccharomyces cerevisiae* and Baculovirus Expression Vector System (BEVS). Experimentally, the expression of bitter taste receptors (TAS2R5, TAS2R7 and TAS2R39) was screened only by recombinantly expressing TAS2Rs in *S. cerevisiae*.

1.1.1. Polyphenols

Phenolic compounds (PC), or commonly referred as polyphenols, comprise a heterologous group of metabolites synthesized by the secondary metabolism of plants [1,14]. These natural compounds are widely present in vegetables, fruits, and derived products (e.g. red wine, green tea, beer, and coffee) [1,15]. *In planta*, their functions range from pigmentation to growth, as defence against predators and infestation by microorganisms [16]. In foodstuffs, these compounds are responsible for several organoleptic features, such as colour and taste properties. Regarding to the latter, astringency and bitterness are perceived in a diversity of foods and beverages such as unripe fruits, wines, teas, and beers [16]. Actually, PC turn out to be associated with several health benefits, having particular biological properties as antioxidants, anticarcinogens or antimutagens, to prevent some cancer, allergies, cardiovascular, Parkinson and Alzheimer's diseases, among others [1,16].

A classic example of the health effects of polyphenols is the "French Paradox", described by Renaud and Lorgeril in 1992 [17]. This paradox has evoked interest to investigate whether antioxidant polyphenols may offer protective effects beyond the cardiovascular system, and whether PC from other plant sources may similarly offer beneficial effects to human health. Despite the high consumption of saturated fat and tabaco, this study revealed a low incidence of cardiovascular diseases, due to a regular and moderate consumption of red wine in the French population [1,17]. Currently, these positive health effects turn out to be associated not only to the strong antioxidant ability of polyphenols but also to complex effects associated to cell signalling [1].

These PC reveal a wide range of structures, from very simple structures (*e.g.*, phenolic acids) through polyphenols such as flavonoids, which contain several groups, to polymeric compounds, according to their complexity [18] (Figure 1). Therefore, polyphenols can be simply classified in two main groups, non-flavonoids, and flavonoids, precisely (Table 1). They can also be subdivided in many sub-classes depending on the number of phenol units in their molecular structure, substituent groups, and/or the bond type between the phenol units (summarized on Table 1) [1,14].

The most simple structures are polyphenols with a single benzene ring (*e.g.*, phenolic acids), compounds with a C_6–C_2–C_6 skeleton with two benzene rings (*e.g.*, stilbenes), and compounds with C_6–C_3–C_6 skeleton, in which the two benzenic rings (rings A and B) are usually linked by a heterocyclic pyran ring (ring C), characteristic of flavonoids (Figure 1). The more complex polyphenols are basically polymers of the structures referred above that contain many different substituents [14,16].

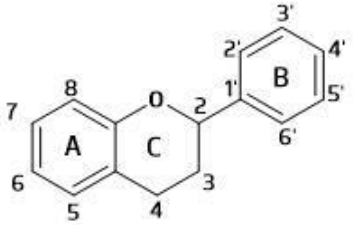

Figure 1. Flavonoids representative structure (flavanic core).

Table 1. Main classes and subclasses of polyphenol compounds.

CLASS	SUBCLASS	EXAMPLES	TYPICAL FOOD SOURCE
NON-FLAVONOIDS	LIGNANS	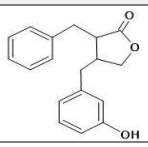 Enterolactone	Linen seeds, broccoli
	STILBENES	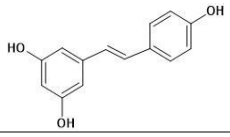 Resveratrol	Red grapes and wine
	PHENOLIC ACIDS	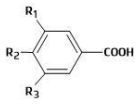 Hydroxibenzoic acid R1, R2= OH; R3= H: protocatechuic acid R1, R2, R3=OH: gallic acid	Coffee, chocolate, spinach
		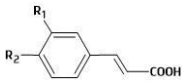 Hydroxicinnamic acid R1, R2= OH: caffeic acid R1= OMe; R2= OH: ferulic acid	
FLAVONOIDS	ANTHOCYANINS	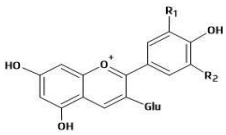 R1= OH; R2= H: cyanidin R1, R2= OH: delphinidin R1, R2= OMe: malvidin	Red fruits, berries
	CHALCONES	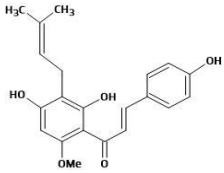 Xanthohumol	Beer
	FLAVAN-3-OLS	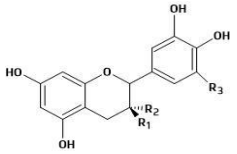 R1= OH; R2, R3= H: (+)-catechin R1, R3= H, R2= OH: (-)-epicatechin R1, R2, R3= OH: (+)-gallocatechin	Red grapes and wine
	FLAVONOLS	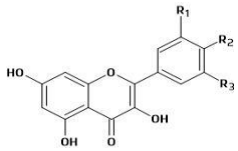 R1, R2= OH; R3= H: quercetin R1, R2, R3= OH: myricetin	Black and green tea; onions
	FLAVONES	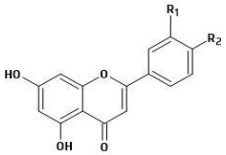 R1, R2= OH: luteolin R1= H; R2= OH: apigenin	Carrot, olive oil and peppers
	ISOFLAVONES	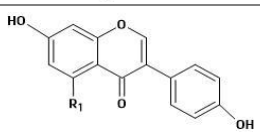 R1= H: daidzein R1= OH: genistein	Soy sauce and milk

Non-flavonoids are characterized by having a single aromatic ring, including phenolic acids, stilbenes, and lignans. The predominant class in this group is represented by small molecules such as phenolic acids (*e.g.*, hydroxybenzoic and hydroxycinnamic acids). These polyphenols are presented in foods such as chocolate, coffee, and spinach [1, 14]. In fact, non-flavonoids commonly exist in their

conjugated form with glucose, quinic acid, structural components of the original plant or even with other polyphenols [14].

Flavonoids are the most important group of polyphenols in food. They are characterized to originate from a central core, the flavanic core (Figure 1) [1]. Flavonoids are classified in various groups according to the oxidation state and substitution pattern of the central pyran ring (ring C) [1, 14]. This structural diversity of flavonoid molecules results in a wide range of compounds that includes flavanones, flavones, flavonols, dihydroflavonols, isoflavonoids, anthocyanins, flavan-3,4-diols, flavan-4-ols and flavan-3-ols [14, 16]. Additionally, there are flavonoids with C_6-C_3-C_6 skeleton without the pyran C-ring in their molecular structure (*e.g.*, chalcones and aurones), which are identified as minor flavonoids. In food, flavonoids appear as glycosides (*e.g.*, fruits, seeds, and vegetables), as aglycones (*e.g.*, tea), or oligomers (as proanthocyanidins, *e.g.*, grapes and peanuts) [14].

Flavonoids can produce several organoleptic responses, from sweet taste (dihydrochalcones) to astringent sensation (proanthocyanidins, flavan-3-ols), and bitter taste (majority of subclasses). Sweet and bitter taste results from the activation of taste receptors on the tongue, whereas astringency is a rough or dry sensation in the mouth. The mechanisms that lead to astringency onset have been a matter of controversy. One of the most important is the interaction between PC and proline rich salivary proteins (PRPs), leading to the precipitation of salivary proteins and loss of lubrication in the mouth [1, 14].

Anthocyanins are responsible for the colors, red, purple, and blue, of various fruits and vegetables (*e.g.*, berries, grapes, black carrots, and red cabbage) and derived products, particularly, red wine. Anthocyanin is considered as one of the flavonoids subclasses, even with the positive charge at the oxygen atom of the C-ring [19]. In fruits, these pigments are always in their glycosylated form, but in other foodstuffs they may appear as aglycon (without the sugar moiety) [1].

The colour and stability of anthocyanins depends on the pH, light, temperature, and structure. In acidic condition, these pigments appear as red and as the pH increases, they turn out to be blue [20]. Apart from the natural dye utility of anthocyanins, these colored pigments provide beneficial health effects as antioxidant, antidiabetic, anticancer, anti-inflammatory, and antimicrobial activities, and in the prevention of cardiovascular diseases. Among anthocyanin group, cyanidin glucoside, delphinidin glucoside, malvidin glucoside, pelargonidin glucoside, peonidin glucoside, and petunidin glucoside are the most common colored pigments distributed in plants [19-20].

Flavan-3-ols are the most structurally complex group of flavonoids, present in fruits, vegetables, beverages, food grains, herbal remedies, dietary supplements, and dairy products [21-22]. They vary structurally according to the stereochemistry of carbon 3 of C ring and to the hydroxylation degree of ring B [1]. These compounds range from the simple monomers (+)-catechin and (-)-epicatechin, which can be hydroxylated to originate gallocatechins (*e.g.*, gallocatechin and epigallocatechin) and also be esterified with gallic acid (*e.g.*, epicatechin-3-*O*-gallate (ECG) and

epigallocatechin-3-*O*-gallate (EGCG)), by complex structures including the proanthocyanidins that are also referred as condensed tannins [21–22].

Table 2. Main classes and subclasses of tannins.

TANNINS			
HYDROLYSABLE TANNINS	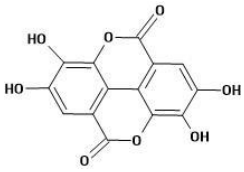	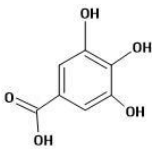	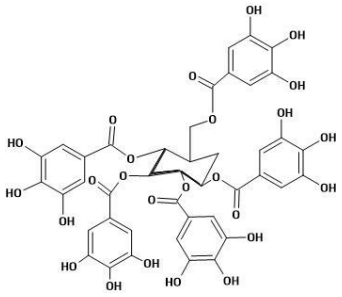
	Elagic acid	Galic acid	Pentagalloylglucose
CONDENSED TANNINS (PROANTHOCYANIDINS)	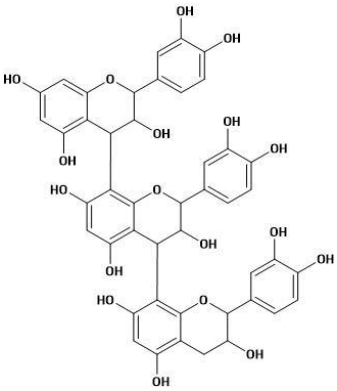	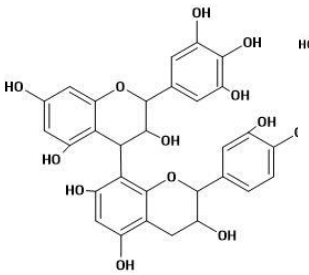	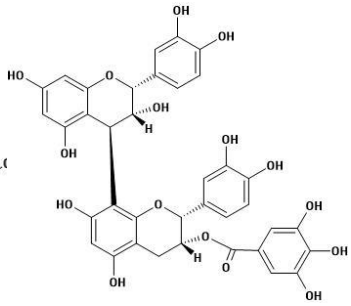
	Procyanidins	Prodelphinidins	Procyanidin dimer B2 gallate

"Tannins" is a term attributed to some polyphenols that have the ability to bind to proteins [1]. According to their chemical structure, they are classically divided in condensed tannins (also referred as proanthocyanidins) and hydrolysable tannins (Table 2). Nevertheless, there are also others minor tannins, essentially, phlorotannins, found in red-brown algae, and complex tannins, result from reactions between gallic or ellagic acids with catechins and glucosides [1,16,23–24].

Proanthocyanidins consists of polymers of flavan-3-ol monomers ranging from dimeric to oligomeric forms and to polymers. According to the hydroxylation pattern of ring B, proanthocyanidins can be divided as propelargonidins (mono-hydroxylated), procyanidins (di-hydroxylated), and prodelphinidins (tri-hydroxylated) [16,23].

Procyanidins are the most common proanthocyanidins and they are built from flavan-3-ols monomers such as (+)-catechin and (–)-epicatechin. Depending on the stereo configuration and linkage between flavan-3-ol monomers, these compounds can be categorized into A-type and B-type. B-type procyanidins are the most abundant and they are identified by a single interflavan bond between C-4 of B ring and either C-8 or C-6 of C ring. The most frequent B-type procyanidins are B1, B2, B3, and B4 that

are C4–C8 type. Regarding to A-type procyanidins, besides their interflavan bond they also have a second ether linkage between the hydroxyl group of A-ring and C-2 of A ring [16,22,25].

Hydrolysable tannins consist of esters of monosaccharides with gallic acid (*e.g.*, gallotannins) or oligomers of gallic/ellagic acids *(e.g.*, ellagitannins) [1, 16, 26]. In food, proanthocyanidins are more common tannins than hydrolysable tannins [16].

1.1.2. Bitter taste

The sensory systems, including the vision, auditory, olfactory, somatosensory (touch, pain, temperature, and proprioception), vestibular (balance, spatial orientation) and gustatory systems have essential roles of presenting the living beings a faithful representation of the external world. As regards to the later, taste perception provides useful sensory information for food appraisal and gives a valuable discriminatory power prior to ingestion [27].

The human being can taste several compounds, but they only recognize five distinct taste sensations, which are (i) sweet, for the detection of sugars and sweeteners, (ii) bitter, for the detection of a variety of alkaloid substances, many of which are toxic, (iii) sour, which detects acids in unripe fruit and spoiled foods, (iv) salty, which perceives sodium and (v) umami, for detection of all L-amino acids in rodents but only *L*-glutamate in humans [27–30]. Nevertheless, taste receptors for canonical taste stimuli have been described, among them are receptors for fatty acid transporters (receptor for fat), for detection of different fatty acids and receptors for kokumi, a stimulus that enhances the basic taste sensations [30].

Taste sense acts as a protector and a guide for our eating habits. The sensations of sweet, umami and salty lead us to prefer foods containing carbohydrates, amino acids, and sodium, while bitter and/ or sour sensations acts as discouragement ingesting poisonous substances and strong acids [30]. These sensations are initially mediated by multiple signaling pathways in the Taste Receptor Cells (TRCs) localized in the oral cavity in the taste buds on the surface of the tongue and palate epithelium [31]. In fact, it is known that different regions of the tongue exhibit different gustatory preferences, and TRCs may selectively respond to different tastants. TRCs, in mammals, are distributed into different papillae, including circumvallate, foliate and fungiform papillae. Circumvallate papillae localized at the very back of the tongue and are singularly sensitive to bitter substances. Foliate papillae are found at the posterior lateral edge of the tongue and are sensitive to sour and bitter compounds. Fungiform papillae are localized at the front of the tongue and mediate the sweet and salty taste quality [27].

The structure of taste buds is similar to that of a garlic bulb and each taste bud contains approximately 50–100 TRCs that have epithelia origin. Based on the morphology of TRCs the cells within a taste bud can be classified into four distinct groups, introduced as type I, II, III that are elongated and spindle shaped, whereas type IV cells are round and all taste buds contain of all four subtypes regardless of their anatomical location [32–34].

Bitter, sweet and umami taste are generally mediated by type II cells, often referred to as receptor cells and, in contrast, sour taste transduction is detected by type III cells. Sweet and umami tastants are perceived by heterodimeric G protein–coupled receptors (GPCRs), namely Taste 1 Receptor (TAS1R), comprising a family of three receptors: taste receptor type 1 member 1 (TAS1R1), taste receptor type 1 member 2 (TAS1R2) and taste receptor type 1 member 3 (TAS1R3). The heterodimeric receptors of TAS1R1 and TAS1R3 subunits are activated by umami tastants and the heterodimeric receptors of TAS1R2 and TAS1R3 subunits are activated by sweet tastants. Bitter tastants are perceived by activation of bitter taste receptors (TAS2Rs, T2R), which are also GPCRs that are expressed on the TRCs. Although, type II taste buds express either TAS1Rs or TAS2Rs, they respond exclusively to either sweet and umami, or bitter tastants [32-33].

Bitter taste perception in humans is mediated by 25 GPCRs of the *TAS2R* gene family. The *TAS2Rs* genes are located on chromosomes 5, 7 and 12. Besides *TAS2R1* gene, which is localized on chromosome 5, all the other genes are ordered on chromosomes 7 and 12. Comparing the *TAS2Rs* gene sequences revealed that genes located on the same chromosome tend to be more closely related to each other than to *TAS2Rs* genes located on different chromosomes [34].

The TAS2Rs are proteins with 290–330 amino acid residues and they can form oligomers. Since humans have 25 TAS2Rs capable to detected thousands of bitter compounds, including peptides, amino acids, lactones, and phenols, among others, it turns to be essential that one receptor responds to more than one compound [1, 28]. TAS2Rs are seven-transmembrane receptors, as they contain seven α-helices passing through the cell membrane. Apart from the seven transmembrane regions, they include three extracellular loops and three intracellular loops. Amongst the 25 TAS2Rs, the extracellular N-termini, and intracellular C-termini, and the lengths of the loops are relatively variable [28].

The number of TAS2Rs subtypes varies in different species, from 3 in chicken to 50 in frog. Even between mouse and human there are different number of TAS2R subtypes. To date it is known that for cat (*Felis catus*), chicken (*Gallus gallus*), and mouse (*Mus musculus*) there are 12, 3, and 35 bitter taste receptors, respectively. The orthology (the homologous sequences evolved from a common ancestor by speciation) between this species is difficult to assign [35]. The chemosensory science explores questions concerning the connection of the habitat and the number of the bitter taste receptors between species. Besides these questions, it also studies the potential existence of different types of bitter taste, the level of overlap between the compounds recognized as bitter by different species, the quest endogenous ligands for extra-orally expressed bitter taste receptors and the chemical features related with extreme bitterness [35].

"Taste receptors" (TAS) were firstly characterized as sensory receptors localized on the tongue, where they are expressed in small clusters of specialized epithelial cells. Nevertheless, many studies reported in recent years an expression of these receptors not only in the oral cavity but

throughout the body and thus to a physiological role beyond the tongue [30]. The main non-gustatory tissues expressing TAS2Rs identified are the gastrointestinal and respiratory tract, playing a role in digestion and metabolism, and act as a warning system for inhalation of harmful substances, respectively [30, 35]. Furthermore, expression of these receptors also has been reported in many other tissues including brain, liver, pancreas, urinary bladder, and testis. The function of TAS2Rs in these tissues has been studied, but in most cases has not been clarified yet [30]. In addition, bitter taste receptors are also involved in the innate immunity aiding on the rapid response of epithelial barrier in avoiding infection at the early stage (*e.g.*, increasing ciliary beat frequency in order to accelerate mucociliary clearance) [35]. This "apparently" chemosensory role in many tissues allows the access to new therapeutic strategies based on the employment of TAS2Rs as potential therapeutic mediators of drug effects [30].

Human bitter taste perception varies significantly showing an individualized perception of different bitter compounds. This feature has been related to single-nucleotide polymorphisms (SNPs) of the 25 TAS2Rs that generate, mainly, modified amino acid sequences, namely haplotypes. In world population, these polymorphisms exist with high frequencies and show to influence receptor activation by bitter compounds. This might affect dietary habits and lead to consequences for an individual's health [1, 29, 35].

1.2. Interaction between food polyphenols and bitter taste receptors

There is an enormous need of new approaches to uncover and understand the bitterness of the different families of compounds, epitopes of binding, the effect of mixtures of compounds, and ways to modulate the TAS2Rs activation. One of the reasons to study the astringency as bitterness molecular mechanisms is toward the development of (natural) strategies to modulate these properties. Nowadays the oldest method to test astringency and bitterness is tasting. Sensory impressions of these two properties are easily confused and require specific and significant training to be reliably distinguished.

Bitterness is one of the five most important sensations since its recognition and aversion allows the protection of animals against poisonous substances, which are often bitter. This is literal for bitter taste, as many toxic plant metabolites taste bitter and, therefore, the analogous receptor molecules perform a required role as warning sensors [34, 36]. Thus, the sense of taste is crucial to the survival and well-being of an individual [28, 34].

Some healthy foods such as vegetables, fruits, and derived products (*e.g.*, red wine and green tea) are also perceived as bitter. Furthermore, polyphenols are a family of compounds widespread in plant-based foodstuffs with a well-known healthy property [12]. Although the existence on an inconsistency on the relation between the bitter taste and polyphenols structure, there are some

studies about the bitter taste of PC, that was showed that bigger molecules tend to be less bitter and more astringent. According to Peleg *et al.* (1999) [37], (-)-epicatechin is more bitter than his stereoisomer (+)-catechin, and these two polyphenols are more bitter than procyanidins trimers. Nevertheless, Hufnagel and Hoffman, reported that procyanidins dimers and trimers are more bitter than (-)-epicatechin, suggesting that polyphenols with higher molecular weight are more bitter [1]. Therefore, the major goal is to reduce bitterness from foodstuffs rich in polyphenols, while preserving the health-promoting properties of polyphenols. To accomplish this, it is essential to determine which of the PC are truly bitter and which of the TAS2Rs are responsible for their detection [12].

In fact, some polyphenols have been already identified as agonists for some TAS2Rs, namely, TAS2R5, TAS2R7 and TAS2R39 (Table 3). In 2013, Soares *et al.* discovered that (-)-epicatechin activates TAS2R4, TAS2R5, and TAS2R39 receptors, and pentagalloylglucose (PGG) also shown to activate TAS2R5 and TAS2R39 receptors [12]. On the other hand, procyanidin trimer and malvidin-3-glucoside stimulated only one receptor, TAS2R5 and TAS2R7, respectively [12]. In particular, tannins were the first natural agonists found for TAS2R5 that display high potency only toward this receptor [12]. The catechol and/or galloyl groups appear to be important structural determinants that mediate the interaction of this receptor [12]. Overall, the EC_{50} values obtained for the different compounds vary 100-fold, with the lowest values for PGG and malvidin-3-glucoside compounds, suggesting that they could be significant polyphenols responsible for the bitterness of fruits, vegetables, and derived products even if they are present in very low concentrations [12].

Table 3. Overview of bitter taste receptors and their respective agonists.

Bitter Taste Receptor	Encoded gene	Chromosome localization	Base pairs (bp)	Amino acids	Molecular weight (kDa)	Known agonists
TAS2R5	*TAS2R5*	7q34	897	299	34	(-) -epicatechin and PGG
TAS2R7	*TAS2R7*	12p13.2	957	318	36.5	Malvidin-3-glucoside
TAS2R39	*TAS2R39*	7q34	1014	338	38.6	(-) -epicatechin and PGG

A recent study, from Soares *et al.* [13], reported an interesting activation pattern from the agonist-receptor interaction. First, distinct compounds activate the same receptor, where TAS2R5 was activated by six polyphenols (procyanidins B1, B4, B7, B2g, EGCG, and punicalagin), and TAS2R7 was activated by four polyphenols (vescalagin, castalagin, punicalagin, and granidin) [13]. Second, different receptors are activated by the same compound. This was shown for EGCG, that activates TAS2R4, TAS2R5, TAS2R39, TAS2R30, and TAS2R43 [13]. The authors antecipated that TAS2R5 and TAS2R7 are preferably activated by condensed tannins and hydrolysable (ellagi)tannins, respectively [13]. These activation studies were carried out by expressing 25 TAS2Rs, individually, in Human Embryonic Kidney 293T (HEK293T) cells stably expressing the chimeric G protein Gα16gust44. This cell-based assay is a heterologous expression method based on intracellular calcium release assessed by fluorescent dyes

[12-13]. Cells transfected with TAS2Rs DNA expressing the respective proteins, are incubated with a calcium sensitive fluorescent dye (*eg.*, Fluo-4 acetoximetilester), and then bitter compounds are added. Upon activation of the bitter taste receptors (with phenol compounds), the heterodimeric G-protein couples with the receptor. Subsequently, the heterodimeric G-protein dissociates into $G\alpha_{16}$ and the $G\beta\gamma$-subunit, which initiates the signalling cascade that results in intracellular calcium release. Receptor activation can be registered by a Fluorescence Imaging Plate Reader (FLIRP). To determine dose-response curves of a bitter receptor agonist, the activation of the respective TAS2R is measured at different concentrations, and the half maximal activation concentration (EC_{50}) and maximal receptor activation by the respective agonist can be obtained [13, 38].

To better understand the interaction between polyphenols and these bitter taste receptors, large amounts of protein are required. Notably, one of the major problems in obtaining functional GPCRs is their low expression in natural tissues, which makes it difficult to obtain sufficient amounts of proteins for the activation screening. To overcome this problem, it is essential to establish a heterologous overexpression system for TAS2Rs [39]. Recombinant protein production is typically motivated by an intention to determine the protein structure, explore its activity or search for interaction partners to unravel its form of action [40]. It is important to refer that, when it concerns to produce recombinant proteins, the simplest or most accessible system that satisfy minimum requirement is usually chosen for initial expression studies and if successful these efforts are then scaled up for downstream applications [41]. There are a wide range of methods and expression hosts available for heterologous recombinant proteins production. These include methods in bacteria, yeast, insect, and mammalian cells [41-42]. This last system is commonly used in interaction studies between bitter taste receptors and polyphenols in HEK293T cells, as previous described. However, there are few limitations of working with human cells as high costs for protein production, slow cell growth, expensive media and reagents and culture conditions, such continuous CO_2 supply [43]. Therefore, it is important to attempt the other systems to determine which method is the most suitable to express TAS2Rs maintaining their functional properties. A widely used approach to study the bitterness of compounds *in vitro* used is a heterologous expression system. The workflow is divided in: i) expression and isolation of TAS2Rs, and ii) study interaction between proteoliposomes and test compounds.

1.2.1. Expression and isolation of TAS2Rs

1.2.1.1 Bacteria expression system

Bacteria are commonly the first type of system used to produce longer peptides or complete proteins, as results in high yields in a short period of time and the cells can be propagated with nearly little effort [41]. *Escherichia coli* is the most commonly used bacteria [42]. There are several advantages

offered by *E. coli*, *e.g.*, fast growth (short generation time (20 min.), easy manipulation, cost-effectiveness, high expression levels, functional product with high yield and purity [44-45]. However, if the structure and/or function of the recombinant eukaryotic proteins depend on chaperone systems, proteolytic cleavage, or any other post-translational modification (*e.g.*, glycosylation), *E. coli* is less feasible to be the ideal host. Overproduction of such specimens then requires an eukaryotic expression system [41-42].

1.2.1.2 Yeast expression system

Yeast has been one of the most successful heterologous overexpression system in producing eukaryotic membrane proteins. Yeasts, such as *Saccharomyces cerevisiae* and *Pichia pastoris*, integrate the simple and inexpensive abilities of eukaryotic cells, by increasing the probability of proper folding and having the machinery for many post-translational modifications [39, 41, 46]. This feature is exploited when foreign proteins are expressed in yeast in order to study their function *in vivo*. Especially, *S. cerevisiae* is an attractive expression system as its ability for high level protein production, including integral membrane proteins, its easy and generally low-cost manipulation. It is noteworthy that the glycosylation machinery in yeast differs significantly from human cells, ending in hyper-glycosylation which can mask the active sites of enzymes and weaken their activity [41]. Also, its genome is well-characterized (approximately 12052 kb), as well as the availability of a large number of cloning vectors for the expression of foreign genes, and the short generation time (approximately 90 min) in complete YPD media. Notably, the generation time in synthetic media is approximately 140 minutes during the exponential phase [47-48]. Yeast optimal culture conditions are in a neutral or slightly acidic pH, under aerobic conditions, with an adequate nutrient supply, at the optimal temperatures of 26 to 30°C [49]. Yeasts are chemoorganotrophs, so they use organic compounds as a source of energy. Yeasts preferentially use a wide range of sugars (*e.g.*, glucose, fructose) as source of carbon and energy. Glucose is the main carbon and energy source [50]. Curiously, sugars such as sucrose, maltose or galactose are not metabolized in the presence of glucose [51].

Yeast cells in culture follow a certain pattern of growth than can be divided into four phases as *lag*, *log*, deceleration and stationary (Figure 2). In the course of *lag* phase, no cell growth occurs, but since cell starts actively metabolizing nutrients, DNA replication begins and, subsequently, cell division occurs [52]. Therefore, cells enter into the logarithmic phase. As cell number increase and glucose becomes limiting, cell growth begins to decelerate reaching the stationary phase, where cells stop dividing [53]. Cellular growth is mostly a result of protein production, occurring continuously during the cycle [54].

David Drew and co-workers (2008), developed a protocol for rapidly screening and purifying eukaryotic membrane proteins in the yeast *S. cerevisiae*. They mentioned that using this protocol, within 1 week many genes can be rapidly cloned by homologous recombination into a GFP-fusion vector and their overexpression efficiency was determined using whole-cell and in-gel fluorescence [39]. As is evident from the studies of four GPCRs the use of a yeast expression system has been successfully used to determine their structure (*i.e.*, rhodopsin, turkey β1-adrenergic, human β2-adrenergic and human adenosine A2a receptors) [40].

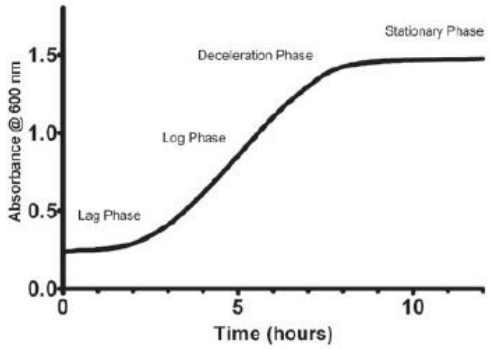

Figure 2. Classical yeast growth curve. *S. cerevisiae* grown in YPD media at 30°C for 12 hours with OD_{600} measurements every 2 minutes. (Adapted from *Held*, 2010)

S. cerevisiae also has the added advantage of having a highly regulated and extensively characterized quality-control system in the endoplasmic reticulum (ER), hence assessing localization of fusions under overexpression conditions can be used as a good indication of functional expression [39, 46]. In 2009, Sugawara and colleagues screened the expression of 25 TAS2Rs in *S. cerevisiae* using a GFP-fusion expression system. This study revealed that after optimization only five TAS2Rs, in which one of them was TAS2R7, were expressed at levels greater than 1 mg protein/L culture, which is a preferable level for protein purification [46]. The same study conclude that the fusion of the N-terminal sequence of the STE2 receptor into the TAS2R constructs, increased only TAS2R5 expression, with an increase of 2.2-fold, suggesting that the use of an additional protein expression-enhancing signal sequence might be unnecessary for all TAS2Rs [46].

Drew and colleagues also reported that, due to a lack of certain lipids (*e.g.*, cholesterol), membrane proteins that express well in yeasts may in some cases need to be produced in insect or mammalian cells for functional or structural works. Nevertheless, because of its speed and comparatively low cost, *S. cerevisiae* remains a valuable pre-screening host even in such situation [39].

1.2.1.3 Insect expression systems

Insect expression systems perform an adequate compromise between the bacterial and mammalian systems. In insect cells, signal peptides are cleaved as in mammalian cells, disulfide bonds are formed in the endoplasmic reticulum and proprotein-converting enzymes are available for proteolytic processing. Comparing with the wide range of expression hosts available for heterologous recombinant protein production, insect cells are ideal for producing complex proteins that require vast post-translational modification. The established insect cell lines used to produce recombinant proteins grow to higher densities than mammalian cells, hence smaller culture volumes are enough. Although insect cell cultures are less demanding than mammalian cells (*e.g.*, no need for CO_2 atmosphere), keeping of sterility is equally important [41]. Normally, insect cells infection is carried out with a baculovirus vectors [41].

In this thesis, besides the yeast expression system, the chosen insect cell system was a Baculovirus Expression Vector System (BEVS). This system is widely used to produce recombinant proteins in insect cells and has been broadly reviewed [55-58]. It is usually suitable for co-expression of heterologous genes for producing multi-protein complexes or to provide specialized proteins for enhanced processing (*e.g.*, chaperones). Baculovirus are a large, diverse group of viruses that specifically infect arthropods (*e.g.*, moths and butterflies) [41]. As insect cells are higher eukaryotes, they can properly do post-translational modifications. Besides that, the huge and flexible viral genome (~130 kb) used allow a high capacity for multiple genes or a large insert insertion. Also important, the virus used does not replicate in human cells and a very high yield is normally obtained driven by the strong promoters (*e.g.*, polyhedrin or p10) [41, 59-60].

1.2.1.3.1 Baculovirus life-cycle

Autographa californica multiple nuclear polyhedrosis virus (AcMNPV) is the most well studied baculovirus. AcMNPV life cycle comprises two phases leading to different phenotypes, including budded virus and occlusion-derived virus (Figure 3.). Budded virus is enveloped with parts of the host cell membrane, and after its release from the host cell between the early and late phases of the infection, they can spread and infect adjacent cells. Occlusion-derived virus are produced in the very late infection phase when the viral protein polyhedrin accumulates in the host cell and forms so-called occlusion bodies [41].

The promoters used for heterologous gene expression with BEVS are commonly viral promoters, and these can be categorized as early (0–6 hours post-infection, hpi), late (6–24 hpi) and very late promoters according to the timing of their activity post-infection. Early phase takes 0 to 6 hours post-infection (hpi), late phase stand for 6 to 24 hpi, and very late phase proceed the next 18–24 to 72 hpi. The protein expression is controlled by the strongest viral promoter, the *polh* promoter. The *polh* promoter is the most widely used in BEVS because of its very high activity and since occlusion body formation (and thus polyhedrin itself) is not necessary for baculovirus propagation in cell culture [41, 61].

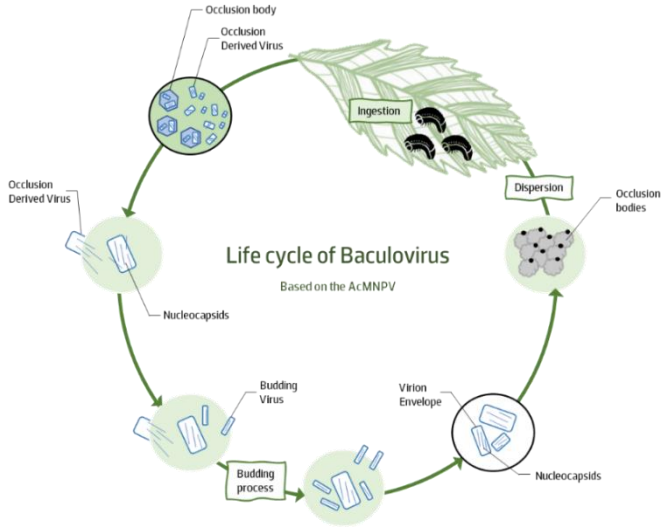

Figure 3. The lifecycle of baculovirus. Baculoviruses have a biphasic life cycle where two different forms of the virus. Infection between hosts is mediated by virions occluded in occlusion bodies late in infection. (Adapted from Chambers *et al.*,2018)

1.2.1.3.2 Generation of recombinant viruses

Before cell infection, the first step is to insert the gene of interest into a transfer vector downstream of the polyhedrin promoter next to gentamycin resistance gene. The virus genome present in *E. coli* cells (*e.g.*, DH10MultiBacTurbo or DH10EMBacY cells) must recombine with the transfer vector, generating the bacmid (recombinant baculovirus). The gene of interest is introduced into the transfer vector with a viral promoter (*e.g.*, the polyhedrin promoter) flanked by viral DNA sequences matching the target locus [41]. The viral DNA sequences that flanks the polyhedrin promoter are the right and left arm of the Tn7 transposon (Tn7R and Tn7L, respectively), which forms a mini-Tn7 element. The bacmid carries a mini-*att*Tn7 target site into which the mini-Tn7 from the acceptor vector is inserted by site-directed transposition (Figure 4). The bacterial cells containing the bacmid also provide a helper plasmid encoding the Tn7 transposase, that carry out transposition following transformation of the cells with the acceptor plasmid. Colonies containing bacmid carrying the insert (transgene) are identified by blue/white screening [62]. This selection procedure is made by replacing the polyhedrin gene of the parental virus with the bacterial *lacZ* gene, and consequently cells containing parental virus form blue colonies in the presence of a chromogenic substrate such as X-Gal, while

successful recombinants form white/colorless colonies where Tn7 transposition disrupts expression of the lacZ peptide, plus gentamycin resistance, and optionally through selective resistance markers (*e.g.*, kanamycin and tetracycline) [41, 62].

1.2.1.3.3 Bacmid and baculovirus expression

First introduced in 2004, the MultiBac system has been significantly reengineered to increase protein production and reduce protein degradation. Thus, in 2011, Craig and Berger, updated the ACEMBL Expression System Series Multibacturbo for multi-protein expression in insect cells. The MultiBac^{Turbo} and EmBacY baculoviral genomes have, approximately, 130 kb and are derivatives from *Autographa californica* nucleopolyhedrovirus (AcMNPV) (Figure 2).

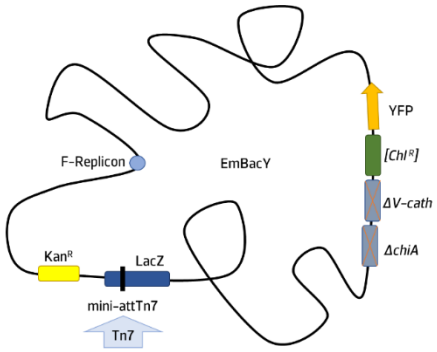

Figure 4. Schematic representation of EmBacY baculoviral DNA. The Tn7 attachment site is located inside the *LacZ* gene, where occur insertion of Tn7 elements from recombinant pACEBAc1. (Adapted from Berger *et al.*, 2011)

To improve the cell compartments maintenance throughout infection and protein production, two baculoviral genes, *v-cath* and *chiA*, were disrupted. The *v-cath* gene encodes for a viral cathepsin-type cysteine protease, V-CATH, activated after cell death through a process that depends on juxtaposed gene on the viral DNA, *and chiA*, encodes for a chitinase. These two genes are involved in the liquefaction of the host insect cells. The disruption of these two genes served to- eliminate V-CATH activity and to enable chitin-affinity chromatography for purification without interference *from chiA* gene product. The deleted viral DNA sequence was replaced with a LoxP sequence, which allows *cre-lox* site-specific recombination. However, in MultiBac^{Turbo}, the target construct it is not introduced on the LoxP site. Alternatively, the gene of interest is transferred into the bacmid via transposition into the mini Tn7 attachment site [62-63]. The LoxP site was then reengineered and a Yellow Fluorescent Protein (YFP) gene was integrated to generate EmBacY bacmid. This baculoviral genome does no longer allow the accession on the LoxP site in the virus backbone through co-expression of Cre. The YFP insertion as a marker was particularly useful for monitoring the fluorescence signal or just by looking at the color of the culture turning greenish, indicating when cultures need to be harvested to obtain best results [62-66].

After purification of recombinant bacmid DNA from the selected clones, insect cells can be transfected to produce recombinant viruses [41].

1.2.1.3.4 Cell lines for Bacterial Infection

BEVS is commonly used with cell lines Sf-9 and Sf-21, originated from cell line IPLB-SF-21 isolated from *Spodoptera frugiperda* pupal ovarian tissue, as well as BTI-TN-5B1-4, settled down from ovarian cells of the cabbage looper *Trichoplusia ni*, better known as High Five™. Sf-9 were identified as a denser as faster-growing subclone of Sf-21. Regarding to BEVS, High Five™ cell line achieves the highest yield, while Sf-9 and Sf-21 productivity was less sensitive to cell density [41, 62].

1.2.1.3.5 Determination of baculoviral expression

Since protein expression in the baculovirus system is induced by the late to very late polyhedrin promoter, the protein expression onset will exhibit some lag and should be expected to initiate yielding significant amounts at 15 to 24 hours post-infection (hpi). The expression peak may vary, but it is presumably to be around 40 hpi. To determine the expression peak, it is required rapid and reliable methods. Expression of target genes from recombinant yeast plasmid and EmBacY bacmid can be analyzed by SDS-PAGE with or without subsequent Western-blot. The addition of tags allows purification of proteins [41].

1.2.1.4 Protein detection

Ideally, the production of recombinant proteins would be done without modification or expansion of the original polypeptide sequence and this is achievable if the native protein can be detected and isolated using current tools (*e.g.*, antibodies for purification or mass spectrometry for identification). Even without these tools, the purification of an unmodified protein could be carried out if the yield were sufficient for identification by SDS-PAGE followed by non-specific staining. However, adding an affinity tag or even a fusion protein turns the process of protein detection and isolation more straightforward by using standard procedures such as affinity chromatography, and this way allowing for a more efficient purification. In some cases, the additional polypeptide sequence may increase the yield for stability, or by reducing toxicity [41].

Fusion tags- amino acid sequences that are genetically coded to be expressed as attached moieties to a protein. Commonly used fusion tags include the polyhistidine tag (His-tag), FLAG-tag, Strep-tag, GFP-tag, among others [41, 62]. Six to ten consecutive histidine residues (His_6 to His_{10}) are used frequently as an affinity tag, which allows the purification of His-tagged recombinant fusion proteins with an anti-polyhistidine antibody or more often by Immobilized Metal-Ion Affinity Chromatography (IMAC) [41, 46]. To improve the success in obtaining pure membrane proteins GFP-based fusion method is commonly applied as a reporter protein. As the C-termini GFP folds and becomes fluorescent only if the upstream membrane protein integrates into the membrane, it turns out to be a fast and accurate measure of membrane-integrated expression. The advantages for using this approach is that fluorescence is easy to measure directly from a liquid culture, standard SDS-gels, and detergent-solubilized membranes.

The GFP-tag remarkably speeds up detergent screening and purification. Detergent-solubilized membranes can also be subjected to fluorescence size-exclusion chromatography (FSEC) to measure the "monodispersity" of the sample. Although there is no guarantee of maintaining the functionality of the membrane-integrated expression, the GFP-tag helps to obtain stable and homogeneous material for functional and structural works [46, 59]. Another fusion tag that provides rapid one step affinity purification is the Strep-Tag II, which is a short peptide comprising eight amino acids (sequence: WSHPQFEK). This sequence can be fused to recombinant proteins at the N- or C-terminus and demonstrate intrinsic affinity into Strep-Tactin. Affinity purification of Strep-tag II depend on highly specific interaction between Strep-tag II and Strep-Tactin resin, with reducing non-specific interaction by other host proteins and allowing to obtain highly pure recombinant proteins [67].

The presence of the GFP-His tag allows expression levels to be estimated by GFP-fluorescence of the whole cell. Afterward, the integrity of the GFP fusion protein can be confirmed by Western-blot using standard SDS-PAGE [39]. This system also allows rapid assessment of stability and monodispersity of the fusion proteins in detergents. This is performed using fluorescence size-exclusion chromatography (FSEC) without the need for extensive purification [68-69]. It was also reported that the FSEC profiles of the fusion proteins and SEC profiles of the purified proteins are similar [68], indicating that FSEC conditions (i.e., detergent concentration, buffer content, etc.) may be suitable for the final protein purification. Sugawara and colleagues, in 2012, evaluated the detergent (DDM) solubilization efficiency and FSEC of the TAS2R-GFP fusion proteins. These experiments were performed with and without CHS to test its effects on stabilizing the receptors. They verified that DDM solubilization efficiency yield increased when combined with CHS. Drew et al. 2009 recommended to add detergent and CHS at a final concentration of 1% and 0.2%, respectively [39, 46].

1.2.1.5 Bitter Taste Biosensor (BITS)

The current knowledge of bitter taste will be the basis for the Bitterness Biosensor (BITS), a method that will make use of the actual taste cells components, to allow for the assessment of bitter taste properties by the TAS2Rs assembled into proteoliposomes. Biosensor systems, *e.g.* proteoliposomes, are capable of detecting analytes upon interaction between protein and ligands and are gaining attention as useful tools for biotechnological applications. Proteoliposomes have a key advantage since they can be obtained with a small number of lipidic (and protein) components, facilitating the design and interpretation of experiments [70]. The existent taste sensors use physicochemical methods performing well in simple test systems (e.g., one compound) and for known bitter molecules [70-71]. But for detection of new bitter or bitter masking compounds, these sensors are only of limited value since they are based on very different physicochemical mechanisms compared to taste cells [70].

Incorporation of TAS2Rs into liposomes seems a promising approach toward bitter taste biosensors (BITS). However, it is crucial to control if the proteins retain their previously observed interaction patterns with food bitter molecules. Moreover, the validation should include complex mixtures of compounds to determine the use of this biosensor in complex mixtures. The study of biosensors interactions with bitter molecules requires physicochemical techniques, such as, e.g., STD-NMR, fluorescence quenching, microcalorimetry, to characterize the interactions at molecular level [72-74]. This will allow determining binding constants, epitopes of binding, type of bonds involved, and thermodynamic parameters. Understanding the molecular features of the interactions will allow a planned and directed strategy of modulation with specific approaches.

1.2.2. Screening of TAS2Rs activation by polyphenols by an engineering GPCR-based signaling in *S. cerevisiae*

The primary method that eukaryotes use to respond to specific signals in their environment is by GPCR signaling. Prediction of the association between stimulus and response for each GPCR revealed to be difficult due to variety in natural signal transduction architecture and expression. Therefore, April last year, Shaw and colleagues introduced a GPCR-based signaling in yeast that enables the prediction of tuned response to stimuli using synthetic tools. They built a model strain keeping only the core signaling elements, which was an extensively studied mitogen-activated protein cascade kinase (MAPK) signaling cascade. This signaling pathway in *S. cerevisiae* allows to build systems for developing GPCRs to desired targets or to couple heterologous GPCRs to yeast gene expression. Although mammalian systems still are the go-to choice for studying GPCR activity, yeasts are easy to use and have low costs turning this system an ideal organism for many sensor applications [75]. Besides the few limitations of using yeasts as an organism host, the main advantages of this new signaling system, with an engineered *S. cerevisiae* strain, is that it does not require TAS2Rs isolation and allows the induction of these receptors expressed in yeast cells with a variety of ligands [75]. For these reasons, this method was also selected to screen the activation of the TAS2Rs with a list of polyphenols.

In summary, there are few studies that have investigated the structure-activation association of TAS2Rs to polyphenols. So, the main goal of this thesis was to develop systems of heterologous expression to obtain TAS2Rs, TAS2R5, TAS2R7, and TAS2R39, and then study their interaction with a library of polyphenols, some of which already have been described as bitter compounds.

2. Materials and methods

2.1. Yeast expression system for bitter taste receptors

2.1.1. Strains and growth condition

S. cerevisiae FGY217 (*MAT*α, *ura3-52, lys2Δ201, and pep4Δ*) and yWS677(*S. cerevisiae* BY4741 derivative – *sst2 Δ0 far1 Δ0 bar1 Δ0 ste2 Δ0 ste12 Δ0 gpa1 Δ0 ste3 Δ0 mf(alpha)1 Δ0mf(alpha)2 Δ0 mfa1 Δ0 mfa2 Δ0 gpr1 Δ0 gpa2 Δ0*) strains were kindly provided by Dr. David Drew (Stockholm University, Sweden) and by Dr. Tom Ellis (Imperial College, London), respectively. FGY217 strain lacks the *pep4* gene, which encodes for vacuolar endopeptidase Pep4p. This deletion not only inhibits Pep4p protease but also reduces the levels of vacuolar hydrolases. Cells were grown in YPD media at 26°C, 220 rpm, and transformation was carried out using the lithium acetate method (Drew *et al.* 2008) [39].

2.1.2. Preparation of TAS2R_pRS426_*Sma*I vectors

Vector pRS426_GAL1_GFP was kindly provided by Dr. David Drew (Stockholm University, Sweden). The cDNA for TAS2R5, TAS2R7 and TAS2R39 were obtained from Twist Bioscience. The individual TAS2R genes were then amplified from the respective cDNA by Polymerase Chain Reaction (PCR). The genes encoding TAS2R7, and TAS2R39 were cloned into the vector pRS426_*GAL1*_GFP, and TAS2R5 was cloned into the vector pRS426_*GAL1*_STE2_GFP (Figure 5), resulting in plasmid TAS2R7-GFP, TAS2R39-GFP, and TAS2R35-GFP, respectively. The vector pRS426 carries the inducible *GAL1* promoter, harbouring the gene sequence for yeast-enhanced GFP (yEGFP), an octa-histidine tag (His_8-tag), and a URA selection marker.

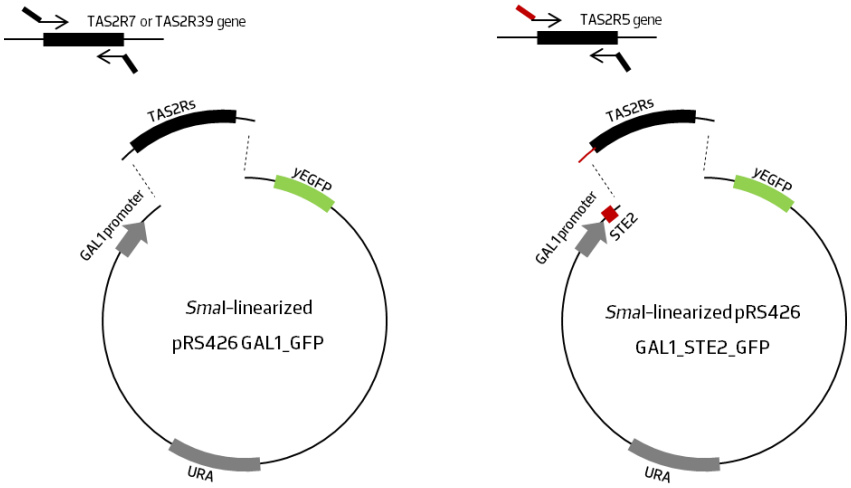

Figure 5. Schematic representation of vectors used to express TAS2R-GFP fusion proteins in *S.cerevisiae* FGY217. TAS2R7 and TAS2R39 were cloned via homologous recombination into *Sma*I-linearized pRS426 GAL1-GFP vector (A) and TAS2R5 was cloned into *Sma*I-linearized pRS426 GAL1-STE2-GFP vector (B). Expression of these three TAS2Rs was screened by yeast-enhanced green fluorescent protein (yEGFP), galactose promoter (*GAL1* promoter), and uracil selection marker (URA). Adapted from Sugawara *et al.* (2009).

Table 4. List of oligonucleotides used to generate TAS2Rs-GFP fragments for cloning pRS426 vector.

Full-lenght primer	Sequence (5'→3')
TAS2R5_STE2-fwd1	CCT GAG CAA CTT TTA TGA TCC GAC CTA TAT GCT GAG CGC TGG CC
TAS2R5_STE2-fwd2	ACC CCG GAT TCT AGA ACT AGT GGA TCC CCC ATG AGC GAT GCG GCG CCG AGC CTG AGC AAC TTT TAT GAT CCG ACC TAT
TAS2R5_STE2-rvs	AAA TTG ACC TTG AAA ATA TAA ATT TTC CCC TGG GCC CCA GCA TCT CC
TAS2R7-fwd	TCG ACG GAT TCT AGA ACT AGT GGA TCC CCC ATG GCA GAT AAA GTG CAG ACT ACT TTA TTG
TAS2R7-rvs	GAT TTG TTT ATG TTG TTG GAA TTT TCT TCC AAA TTG ACC TTG AAA ATA TAA ATT TTC CCC
TAS2R39-fwd	TCG ACG GAT TCT AGA ACT AGT GGA TCC CCC ATG CTA GGG AGA TGT TTT CCT CCA G
TAS2R39-rvs	CAG AGT CCA CTC TTT TGG GTA AAG ATG AAA TTG ACC TTG AAA ATA TAA ATT TTC CCC

2.1.3. Polymerase chain reaction, PCR

The reverse transcription products, cDNAs, were amplified by polymerase chain reaction (PCR) using Phusion DNA Polymerase (Biochemical and Biophysical Technologies- b2Tech). The PCR was carried out using the following conditions; an initial denaturation step at 98°C for 2 min, followed by 30 cycles of denaturing at 98°C for 30 sec, annealing at 55°C for 30 sec, and extension at 72°C for 1 min and 30 sec (1 min/1Kb DNA size), followed by a single final extension of 10 min at 72°C. The PCR product was kept at 12°C, prior to analysis on an agarose gel. A range of different sets of primers, forward and reverse, were used for PCR. All primers were from Eurofins Genomics (Table 4).

2.1.4. Electrophoresis

All PCR products were analysed using 0.8% agarose gels in 1x Tris-base, Acetic acid and EDTA (TAE) buffer, stained with GreenSafe Premium (NZYTech). 100 pb was the ladder (Solis BioDyne) used in this experiment. The gel was then run at 180 Voltage (V) with constant ampere (A) for 35 min and examined with UV prior to digital capture of the image. The PCR products were gel-purified using the NZYGelpure kit (NZYTech) following the manufacturer's protocol and kept on ice until further use. After purification, DNA quantification was measured by nanodrop (Nanodrop nd-1000 Spectrophotometer).

2.1.5. Plasmid linearization by restriction digestion

pRS426 was digested by *Sma*I enzyme, which gives rise to blunt ends that eliminate background colonies caused by the re-annealing of linearized vector during transformation by heterologous recombination. Digestion was carried out at 37ºC for 2-3h. Then linearization was analysed by an 1% agarose gel, as described in section 2.1.4.

2.1.6. Transformation of gene–vector construct into *S. cerevisiae*

2.1.6.1 Preparation of yeast competent cells

S. cerevisiae FGY217 cells were made competent using the standard lithium acetate protocol (Drew *et al.* 2008). A single colony of *S. cerevisiae* FGY217, grown on a yeast peptone dextrose (YPD) plate, was used to inoculate 2 mL YPD broth in a 50 mL aerated tube and incubated overnight at 26°C, 140 rpm. Next day, the overnight culture was diluted to OD_{600}=0.12 into 10 mL fresh YPD broth in a 50 mL shaker flask. The cells were grown at 26°C, 140 rpm until the OD_{600} reached 0.5–0.6. The cells were then harvested by centrifugation at 3 000 g, 4ºC for 10 min. Supernatant was discarded, and the pellet resuspended with 25 mL sterile water followed by a further centrifugation at 3 000 g, 4ºC for 10 min. The pellet was then resuspended with 1 mL of 100 mM lithium acetate (LiAc) and centrifuged briefly at 8 000 g for 15 s. Finally, the pellet was resuspended in 400 µL of 100 mM LiAc and kept on ice for transformation.

2.1.6.2 Transformation into *S. cerevisiae* FGY217

Transformation was carried out by dispensing 50 µL of the competent cells into 1.5 mL eppendorf tubes containing cold 240 µL sterile 50% (w/v) PEG 3350, 12.5 µL of 2 mg/mL single-stranded carrier DNA, salmon sperm (Sigma) was then added and the mixture vortexed for 5 s. Next, 22 µL of DNA mix (5 µL of 14.4 ng/ µL *SmaI*–digested vector and 17 µL of 46.6 ng/ µL PCR product and for the negative control was 17 µL of sterile water instead PCR product) was added to the competent cells and vortexed for a further 5s. The mixture was then incubated at 30°C for 30 minutes followed by heat–shock at 42°C for 25 min. The cells were pelleted by brief centrifugation at 8000 g for 15s at room temperature and resuspended in 100 µL sterile water. The cell suspension was plated onto a –URA selective plate [2 g/L of yeast synthetic drop–out medium without uracil (Formedium™), 6.7 g/L yeast nitrogen base without amino acids (Sigma), 2% (w/v) glucose, and 40 g/L of bacteriological agar (Sigma)], and incubated at 26°C incubator for 2–3 days.

2.1.6.3 Colony PCR

To evaluate positive colonies, a colony PCR method was performed. All colonies obtained on step 2.1.6.2 were selected and resuspended in 10 µL of sterile water. Then the suspension was incubated at 99°C for 5 min, and then placed on ice until utilization. To each 0.2 mL PCR tube, 50 µL of sterile water was added and transferred a small amount of each colony. The PCR was performed as mentioned before (section 2.1.3). As positive and negative control, gel extracted PCR band (R5_STE2) and empty plasmid (pcDNA3.1), were used, respectively. An electrophoresis 1% agarose gel was performed as mention before (section 2.1.4).

2.1.6.4 Plasmid isolation from *S. cerevisiae* FGY217

To each 50 mL flask, 20 mL of – URA selective broth was added and inoculated 70 μL of three transformants (TAS2R5, 7 and 39). It was incubated at 26°C, overnight at 140 rpm.
Next day, the pre-culture was harvested by centrifugation at 4000 rpm for 10 min at room temperature. Supernatant was rejected, and pellet was washed with 10 mL of sterile water and centrifuged again at the same conditions. Cell pellet was resuspended on 1 mL of ultrapure water and transferred to 1.5 mL tubes, then the cellular suspension was submitted to a centrifugation at 3000 rpm for 10 min. Supernatant was discarded, and pellet was resuspended on 200 μL of Buffer A1 (NZYMiniprep Kit). Glass beads were added, and cell suspension was vigorously vortexed ~20 min. Further steps were performed following NZYMiniprep kit (NZYTech) according to the manufacturer protocol. Quantification of plasmid DNA obtained was measured by nanodrop.

2.1.6.5 Transformation into *Escherichia coli* DH5α

To 50 μL of *E. coli* DH5α competent cells, was added 1 μL of plasmid DNA and rest 20 min on ice. Then a heat shock was performed at 42°C for 45 s, and more 2 min on ice. 600 μL of Luria-Bertani (LB) broth was added and incubated at 37°C for 45 min, with shaking at 220 rpm. Cell were harvested by centrifugation at 5 000 rpm for 2 min. 500 μL of supernatant was discarded, and pellet was resuspended with ~100 μL of supernatant. The suspension was plated on LB media with 100 ng/ μL of Ampicillin and incubated at 37°C overnight.

2.1.6.6 Plasmid isolation from *E. coli* DH5α transformants

The *E. coli* DH5α transformants obtained in step 2.1.6.5 were inoculated in 10 mL of LB broth with 100 ng/ μL of Ampicillin (50 mL flasks) and incubated at 37°C overnight with shaking at 220 rpm. Then, the plasmid DNA was isolated with NZYMiniprep Kit (NZYTech) according to the manufacturer instructions. Quantification of plasmid DNA was measured by nanodrop.

2.1.6.7 Sequencing

The three recombinant plasmid DNAs were submitted to DNA sequencing (GATC Biotech Supremerun, Eurofins Genomics) according to supplier's instructions, to confirm de DNA sequence of the insert, and insert orientation.

2.1.7. Preparation of TAS2R_pRS426_*Sma*I vectors for trasnformation into *S. cerevisiae* yWS677

Vector p416_TEF was kindly provided by Dr. Vitor Ferreira (Yeast Signalling Networks, i3S). The cDNA for TAS2R5, TAS2R7 and TAS2R39 was obtained from Twist Bioscience. The individual TAS2R gene was then amplified from the respective cDNA by Polymerase Chain Reaction (PCR). The genes

encoding TAS2R5, TAS2R7, and TAS2R39 were cloned into the vector p416_TEF. This vector allows constitutive expression of proteins and carries the translation elongation factor 1α *TEF1* promoter, harbouring the gene sequence for yeast-enhanced GFP (yEGFP), and a URA selection marker.

Table 5. List of oligonucleotides used to generate TAS2Rs-GFP fragments for cloning p416_TEF vector.

Full-lenght primer	Sequence (5'→3')
TAS2R5_ fwd	AAGTTTTCTAGAACTAGT GGATCCCCCATGCTGAG CGCTGGCC
TAS2R5_rvs	CTTGATATCGAATTCCTG CAGCCCTGGGCCCCAG CATCTCC
TAS2R7-fwd	AAGTTTTCTAGAACTAGT GGATCCCCCATGGCAGA TAAAGTGCAGACTACTTT
TAS2R7-rvs	CTTGATATCGAATTCCTG CAGCCCGATTTGTTTAT GTTGTTGGAATTTTCTTC CTTTTAG
TAS2R39-fwd	AAGTTTTCTAGAACTAGT GGATCCCCCATGCTAGG GAGATGTTTTCCTCCA
TAS2R39-rvs	CTTGATATCGAATTCCTG CAGCCCCAGAGTCCACT CTTTTGGGTAAAGATG

TAS2Rs cDNAs amplification was carried out as previous described in section 2.1.3, modifying to 25 cycles of denaturation, an annealing gradient at 57/60/62ºC for 1 min. A range of different sets of primers, forward and reverse, were used for PCR. All primers were from Eurofins Genomics (Table 5). p416_TEF was digested by *EcoRI* enzyme, and it was carried out at 37ºC for 2-3h. Then linearization was analysed by an 1% agarose gel, as described in section 2.1.4. Transformation of TAS2Rs in *S. cerevisiae* yWS677 was performed as previously described in sections 2.1.3.1 and 2.1.3.2. To verify the proper sequences of TAS2Rs after homologous recombination, plasmid isolation from recombinant *S. cerevisiae* yWS677, transformation into *E. coli* DH5α, plasmid isolation from recombinant *E. coli* DH5 and sequencing was performed as previous described in sections 2.1.6.4 to 2.1.6.7.

2.1.8. Screening colonies by small-scale expression of TAS2Rs-GFP fusion

TAS2Rs-GFP fusions were expressed using the method described by Drew *et al.* (2008). Three colonies of each TAS2R-yeast transformants from -URA selective plate were used to individually inoculate 10 mL -URA broth [2 g/L of yeast synthetic drop-out medium without uracil (Formedium™), 6.7 g/L yeast nitrogen base without amino acids (Sigma), 2% (w/v) glucose] in a 50 mL aerated tube. The cultures were incubated at 26°C, 140 rpm overnight. Next day, OD_{600} measurement of the overnight cultures was taken and the culture was diluted to OD_{600} 0.12 in a fresh 10 mL -URA broth containing 0.1% glucose instead of 2%. The cultures were then incubated at 26°C, 140 rpm until the OD_{600} reached 0.6, and also collected 5 mL and centrifuge at 3000 rpm at 4°C for 5 min. for negative control (before induction). Supernatant was discarded and the cell pellet were stored at -20°C. 2% galactose was then added into individual tubes to induce protein expression for 22h at 26°C, 140 rpm. After 22h, the cells were centrifuged at 4000 rpm at 4°C for 5 min. Supernatant was discarded and the cell pellet (induction samples and control) were resuspended in 200 µL of Yeast Suspension Buffer (YSB) [50mM tris-HCl (pH7.6), 10% glycerol and 5 mM EDTA]. This screening was performed by measuring GFP fluorescence by Whole-cell fluorescence (WCF) and Immunoblotting.

2.1.9. Whole-cell fluorescence

The 200 µL suspension was then diluted 2x and 10x with YSB buffer, for a final volume of 60 µL, for assessment of protein expression by WCF. The fluorescence was measured using a Spectrofluorometer Fluoromax-4 (Horiba) with emission at 512 nm and excitation at 488 nm (excitation slit width of 5 nm). Whole cell protein expression levels in *S. cerevisiae* FGY217 cells were determined by GFP fluorescence.

2.1.10. Electrophoresis SDS_PAGE

All samples were analysed using 15% SDS-PAGE gels in 1x Running buffer [25 mM Tris-base, 192 mM glycine, and 0.1% SDS], loaded with 2x Sample buffer (Bio-Rad). These samples were heat-shocked at 65°C for 10 min., vortexed and loaded into the gel. The Precision Plus Protein ™ All Blue Standards (Bio-Rad) was the ladder for this experiment. The gel was then run at 20 000 – 30 000 ampere (A) with constant Voltage (V) for 1h – 1h 30min. Then Western-blotting analysis was performed.

2.1.11. Western-Blotting

Whole cell proteins were separated by SDS-PAGE and transferred to a polyvinylidene difluoride (PVDF) membrane using a transfer apparatus according to the manufacturer's protocols (Bio-rad). Transfer was made using a cold transfer system [transfer buffer: 25 mM Tris-base, 190 mM glycine, 20% methanol, pH 8.3, at 4°C) at 100 V for 1 h. Membrane was blocked with 5% non-fat milk powder in 1x TBS-T [20 mM Tris-HCl (pH 7.5), 150 mM NaCl, and 0.1% Tween 20] for 1 h, and incubated with 5 mL of antibody (1:1000 dilution of anti-GFP antibody (affinity purified against GFP, produced in b2Tech) in 3% non-fat milk powder in 1x TBS-T, with constant agitation, overnight at 4°C. Membranes were washed three times for 10 min and incubated with 10 mL of antibody (1:10000 dilution of anti-rabbit IgG antibody (Biotinylated, Cell Signaling Technology, #14708)) in 3% non-fat milk powder in 1x TBS-T, for 1 h at room temperature, with constant agitation. Membranes were washed three times for 10 min and developed with the ECL system (Pierce™ ECL Western Blotting Substrate, Thermo Scientific ™) (1:1). In order to visualize protein bands, an Imaging system (ChemiDoc ™ XRS+, Bio-Rad) with an Image Software (Image Lab™ Software version 4.1) was used.

2.1.12. Screening of optimal expression conditions by small-scale expression of TAS2Rs-GFP fusion

TAS2Rs-GFP fusions were expressed using the method described by Drew *et al.* (Drew *et al.* 2008). The selected clone of each TAS2R-yeast transformant from -URA selective plate were grown with the same conditions described in section 2.1.7. Time, addition of a chemical chaperone and temperature were the expression conditions tested with and without 2% galactose induction for each

TAS2R. To induce protein expression, 2% galactose was added into individual 50 mL flaks. All *S. cerevisiae* cells were induced for 22 h and 44h (time), at 20°C and 26°C (temperature), and with or without 2.5% DMSO (chemical chaperone) at 140 rpm (Table 6). Controls for each expression condition were made by adding 0.1% glucose instead of 2% galactose. After 22h and 44h, the cells were centrifuged at 4000 rpm at 4°C for 5 min. Supernatants were discarded and the cell pellets were resuspended in 200 µL of Yeast Suspension Buffer (YSB) [50mM tris-HCl (pH7.6), 10% glycerol and 5 mM EDTA]. This screening was performed by measuring GFP fluorescence by WCF and Immunoblotting, as described in sections 2.1.9 to 2.1.11. To determine TAS2Rs cell localization, GFP-fusion proteins were monitored by fluorescence microscopy.

Table 6. Optimization of expression conditions for TAS2R5, TAS2R7 and TAS2R39 with and without induction.

Expression conditions with and without induction		
Time (hrs)	Chemical chaperone	Temperature (°C)
22 and 44	2.5% DMSO	20 and 26

2.1.13. Fluorescence microscopy – Staining of yeast cells with concanavalin A

From the 200 µL cell suspension remained from WCF aliquots, that were not diluted, cells were collected by centrifugation at 5000 rpm for 5 min. and cell pellet was washed two times with 150 µL ultrapure water and harvested by centrifugation at the same conditions. Then resuspended with 60 µL of ultrapure water and diluted to an OD_{600} = 0.3, with a final volume of 80 µL. The diluted samples were collected by centrifugation, and the cell pellet was resuspended in the same volume of concanavalin A solution diluted 1:30 with 1.0 M NaCl, with final concentration of 25 µg/mL [76]. After 30 min at room temperature, cells were harvested by centrifugation and cell pellet was washed two times with 500 µL of 1.0 M NaCl and once with 500 µL of ultrapure water, centrifuged and resuspended with the same volume to an OD_{600} = 0.3. The slides were prepared with 40 µL of sample and let dry at 37°C and fixed with 10 µL of 100% acetone. A mounting solution consisting of 9 volumes of glycerol and 1 volume of 0.25 M sodium carbonate-bicarbonate buffer (pH 8.5-9.0, Ibidi Mounting Medium) was employed. Membrane protein GFP-fusion localization in *S. cerevisiae* FGY217 was monitored by widefield microscopy (Leica DMI 600 FFW, LAS X Software).

2.1.14. Isolation and solubilization of TAS2Rs

TAS2Rs clones were grown under selected expression conditions. Cell lysis was performed by disruption with glass beads. Cells were initially pelleted at 4000 x g, for 10 min. at 4°C and resuspended in 1 mL of lysis buffer [50 mM Tris-HCl (pH 7.5), 10% glycerol and protease inhibitor tablets (Roche)]. 1 mL of resuspended cells was then distributed to six 2 mL screw capped tubes and glass beads were added to reach 500 µL. Furthermore, 500 µL of lysis buffer was added to each screw capped tube. Cells were then disrupted using a cell-disruptor Bead-beater (FastPrep 2.4) for 7 cycles of 45 s at 6.5 M/S

velocity, each with an interval on ice for 5 minutes, between cycles. The lysate was centrifuged at 10 000 x g, for 10 s at 4°C (Heraeus Biofuge Primo R Centrifuge, Thermo Electron Corporation) to pellet unbroken cells and cell debris. Supernatant was transferred to an eppendorf. The pellet from the previous centrifugation was resuspended in 500 µL of lysis buffer, and then subjected to another round of homogenization of 3 cycles in FastPrep, followed by an additional centrifugation at 10 000 x g for 10 sec at 4°C. The supernatant was added to the previous supernatant. The total volume of the supernatant obtained was submitted to a centrifugation at 6 000 x g for 10 min at 4°C.

2.1.15. Isolation and solubilization of transmembrane proteins – Method A

Following cell disruption, lysate was transferred to ultracentrifuge tubes. Lysis buffer was added until reach 2/3 of ultracentrifuge tube. The suspension was centrifuged at 120 000 x g (Optima™ XE-100 ultracentrifuge, Beckman Coulter; 70ti rotor), for 1 h at 4°C to isolate cell membranes. The membrane pellets were resuspended in 3 mL buffer B [50 mM Tris-HCl pH 7.5, 1% *n*-dodecyl-β-D-maltopyranoside (DDM; PanReac AppliChem), and 0.2% cholesteryl hemisuccinate (CHS; TCI America)] using a disposable 10 mL syringe with a 21-gauge needle. The membranes were solubilized at 4°C for 1 – 2 hrs with agitation using a nutator. Insoluble material was then centrifuged at 43 000 x g (Optima™ MAX-XP ultracentrifuge, Beckman Coulter; TLA-120.2 rotor) for 40 min. at 4°C.

2.1.16. Isolation and solubilization of transmembrane proteins – Method B

After cell lysis, lysate was incubated with 1 mL buffer B [50 mM Tris-HCl pH 7.5, 1% *n*-dodecyl-β-D-maltopyranoside (DDM; PanReac AppliChem), and 0.2% cholesteryl hemisuccinate (CHS; TCI America)] at 4°C for 3 hrs with agitation using a nutator. Samples were harvested at 15 000x g for 15 min. at 4°C. Binding and elution buffers, samples and HisTrap affinity column (HisTrap HP, 1 mL, Amersham Biosciences) were prepared according manufacturer's protocol. Purification was conducted by applying the prepared sample using a pump (Model EP-1 Econo Pump, Bio-Rad). Binding buffer with 10 mM imidazole was used to wash the column. Elution was carried out by applying elution buffer a different concentrations of Imidazole (50, 150, 300, and 500 mM, respectively). Recombinant GFP-fusion and His-tagged proteins were detected either by SDS-PAGE analysis followed by BlueSafe staining (NZYTech) and Immunoblotting, as described in sections 2.1.10. and 2.1.11, respectively. In this section, immunoblots based on detection of GFP-protein were used to track yields of protein at various steps of cell disruption and solubilization.

3. Results

3.1. Heterologous overexpression and isolation of TAS2R5, TAS2R7, and TAS2R39

3.1.1. Cloning and transformation of TAS2Rs into *S. cerevisiae*

Each *TAS2R* gene was amplified by PCR and cloned into the vector pRS426_GAL1_GFP vector (previously digested with *Sma*I) by homologous recombination in *S. cerevisiae* strain FGY217 (Appendices – Figure 9 and 10).

3.1.2. Screening expression conditions by small-scale expression of TAS2Rs-GFP fusion

Achieving optimal expression of TAS2Rs in yeasts requires maximizing both cell density and the efficiency of induction of expression of the target gene. To determine optimal expression conditions for TAS2Rs, GFP-fusion proteins were screened by measuring, first, WCF, and then analyzing western-blots.

3.1.3. Whole-cell Fluorescence in *S. cerevisiae* FGY217

After measuring fluorescence of cell suspensions (section 2.1.9.), data, from cell suspension dilution 10x with YSB buffer, were analyzed and plotted (Figure 6), representing the total of GFP fluorescence emitted at 512 nm in each sample. To verify the relation between control and the respective induced sample, each expression condition control (absence of induction) GFP signal was considered to be 100%. Analyzing the results from Figure 6, it is possible to observe an increase of GFP signal after 44 hours of induction for all samples in comparison with 22 hours of induction. TAS2R5 and TAS2R39 revealed an increase of expression when these receptors were induced with 2% galactose and 2.5% DMSO at 26°C. However, TAS2R7 show differences between 22 and 44 hours after induction. At 22 hours of induction, this receptor shows an increase of GFP signal when induced with 2% galactose and 2.5% DMSO at 26°C, but at 44 hours of induction an increase of GFP signal when induced at 26°C was observed.

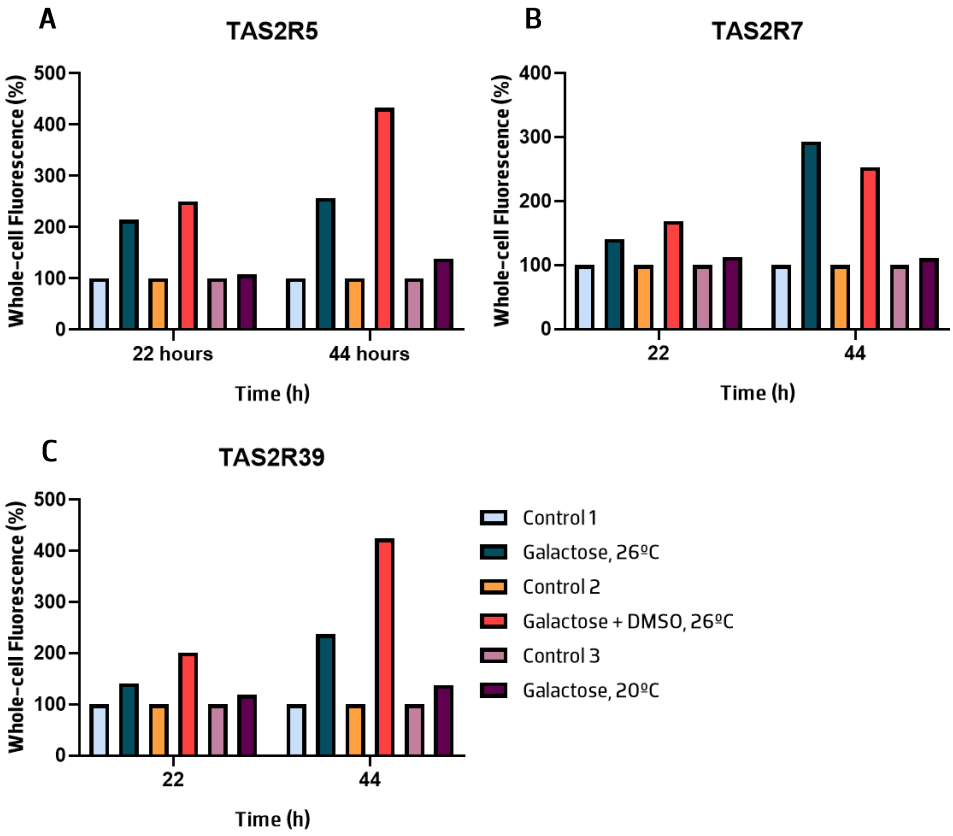

Figure 6. Screening of TAS2R5 (panel A), TAS2R7 (panel B) and TAS2R39 (panel C) expression conditions by WCF in *S. cerevisiae* FGY217. Expression levels were estimated by measuring GFP fluorescence emission at 512 nm by excitation at 488 nm using a Fluoromax 4 spectrofluorometer. WCF was measured before (control 0, represented by black column) and after 22 h and 44 h of induction with 2 % galactose under expression conditions (galactose at 26°C, galactose + DMSO at 26°C, galactose at 20°C, represented by green, salmon, and purple columns, respectively). Induction controls were made by adding 0.1% glucose instead of 2% galactose (control 1, 2 and 3, represented by blue, orange, and lilac columns, respectively).

3.1.4. Immunoblotting

The western blots obtained, for the screening of TAS2Rs expression conditions in *S. cerevisiae* FGY217, are presented in Figure 7 (A1, B1, and C1). These results show the presence of two different bands. One with approximately 47 kDa, the predicted molecular-weight for TAS2Rs-GFP fusion protein (protein of interest), and the other band with approximately 26 kDa the molecular weight of free-GFP protein. From these western blots, GFP- fusion signals were quantified using a densitometer and data obtained was analyzed as shown in Figure 7 (A2, B2, and C2). Results from 44 hours of expression are not shown because it was observed a decrease of expression levels in comparison with results from 22 hours of induction (Appendices – Figure 11). To verify the relation between control and the respective induced sample, each expression condition control GFP-fusion signal was considered to be 100%. Analyzing the results from Figure 7, all TAS2Rs show different optimal expression condition, but all have an increase of GFP-fusion when induced with 2% galactose. TAS2R5 has an optimal temperature condition at 20°C, when TAS2R7 and TAS2R39 have an optimal temperature condition of 26°C Additionally, TAS2R39 show better results when 2.5% DMSO was added.

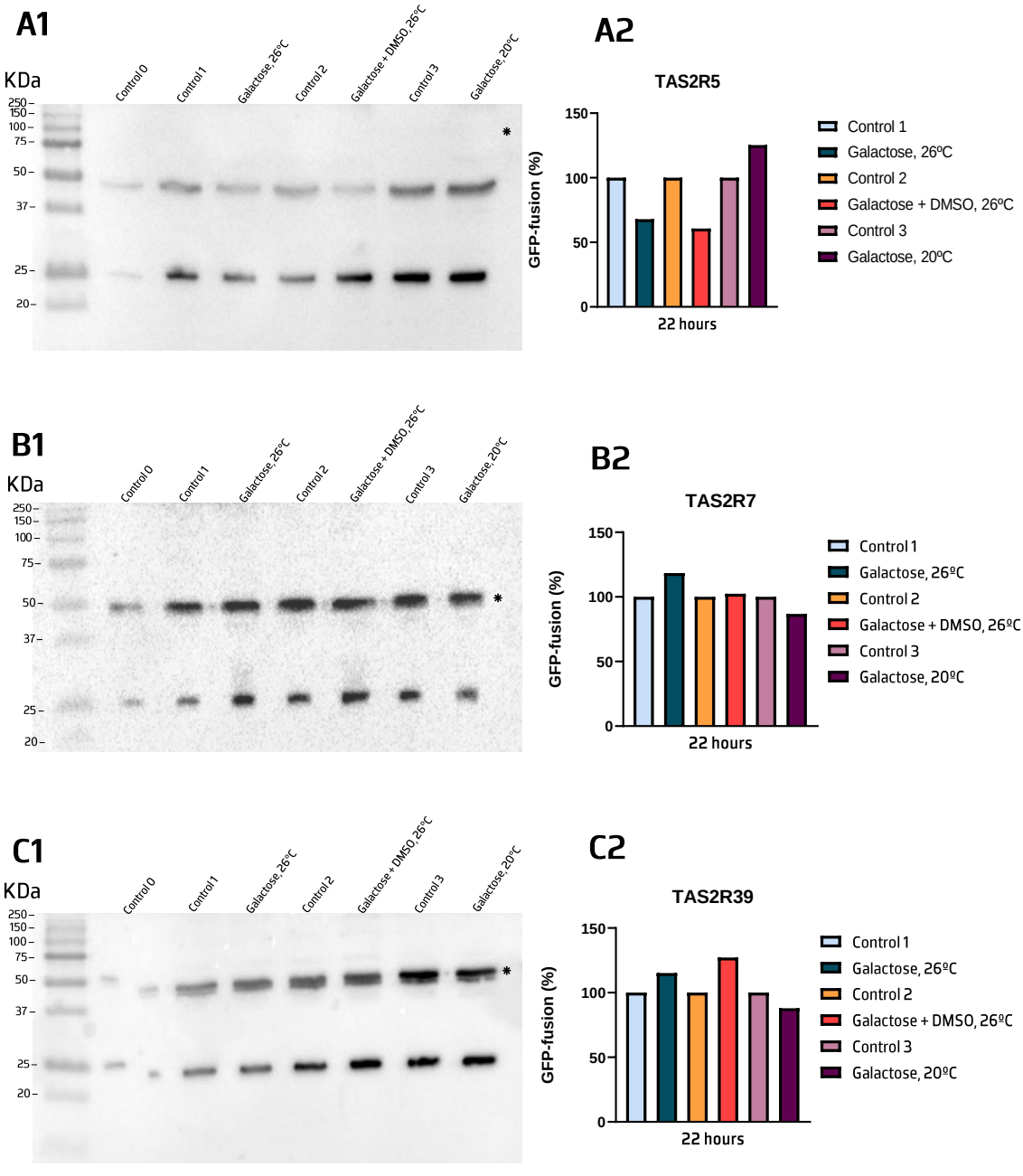

Figure 7. Screening of TAS2R5 (A1), TAS2R7 (B1) and TAS2R39 (C1) expression by Western blotting in *S. cerevisiae* FGY217. Asterisks (*) indicate the bands for TAS2R-GFP fusion proteins, 47 KDa approximately. GFP-fusion signals quantified in a GS800 densitometer with the Quantity one 1-D Analysis Software (A2, B2 and C2). 44 hours expression is not shown because expression levels observed were lower than 22h tested. Lane control 0 (Black column) indicates cell suspension before induction. Lanes Galactose 26°C, Galactose + DMSO 26°C, and Galactose 20°C (Green, salmon, and purple columns, respectively) indicate cell suspension after 22h of induction with 2 % galactose under expression conditions. Control 1, control 2 and control 3 (Blue, orange, and lilac columns, respectively) indicate cell suspensions without induction (0.1% glucose) under expression conditions.

3.1.5. Fluorescence microscopy

To determine TAS2Rs cell localization, GFP-fusion proteins were monitored by fluorescence microscopy (Figure 8). This method was performed with concanavalin A to contrast cell wall to be possible to visualize GFP-fusion proteins, in the cell membrane of *S. cerevisiae*[76]. However, apparently all cell compartments, from all samples including the control (Figure 8 – A to D), were marked with GFP being difficult to determine TAS2R localization. These results might be related with the presence of free GFP in yeast cells, as it was observed in the Western blots results (Figure 7) that this protein leads to great fluorescent signal background.

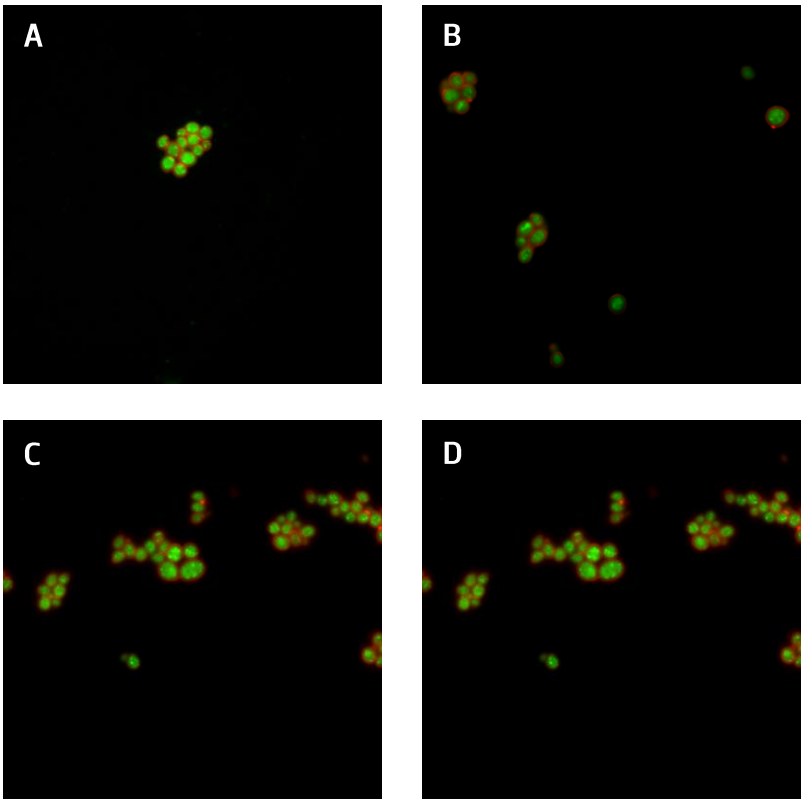

Figure 8. Membrane protein GFP-fusion localization in *S. cerevisiae* FGY217 monitored by widefield microscopy (Leica DMI 600 FFW, LAS X Software). 22 hours induction TAS2R5 (A), TAS2R7 (B), TAS2R39 (C) and *S. cerevisiae* FGY217 (D, control). GFP protein marked by GFP (green fluorescence protein), and membrane cell marked by concanavalin A (red fluorescence).

3.1.6. Isolation and solubilization of TAS2Rs

Both methods (A and B – sections 2.1.15 and 2.1.16, respectively) have given similar results. Isolation of TAS2Rs was tested by yeast cell lysis, fractionation, and solubilization (method A- membrane fraction), or by yeast cell lysis, solubilization and purification (method B- whole cell) of these transmembrane proteins and it revealed to be difficult to obtain membrane fractions isolated from cell debris as the majority of GFP-fusion proteins appeared in conjunction with the unbroken cells in the pellet after performing the homogenization cycles (Appendices- Figure 12).

4. Discussion

Bitterness of polyphenols compounds is an interest topic for consumer's food acceptance and choices, and also for health protection based on food phytochemicals. So, the present study intended to determine if the three TAS2Rs selected were able to be functionally expressed by an yeast expression system, then isolated and purified to incorporate them into liposomes to study their interaction with polyphenols. Furthermore, it is also intended to screen TAS2Rs activation by measuring GFP fluorescence on an engineered *S. cerevisiae* strain that allows exploration of signaling properties and creation of synthetic responses to a range of ligands.

As it is mentioned before, it has been proven difficult to obtain transmembrane proteinsin quantity because their expression levels are very low in natural tissues and there are not sufficient quantities of eukaryotic membrane proteins for structural or functional studies [39]. So, to obtain increased amounts of these type of proteins it was established a heterologous overexpression system, that consists in producing the recombinat protein of interest into a host organism. For that purpose, the three bitter taste receptors were initially expressed using a GFP-fusion yeast system, which was the simplest and most accessible system that satisfied the minimum requirements for this study [41, 46].

To facilitate the expression of TAS2Rs for functional studies, the pRS426 expression vector was selected according the following properties: i) It allows rapid insertion of a given PCR amplified target gene into the vector, following digestion of the vector with a single restriction enzyme; ii) It allows for expression under control of the inducible *GAL*1 promoter; iii) It creates fusions of target gene to C-terminal affinity tags consisting of GFP-His_8 sequences. The use of the GFP-His_8 tags allows the use of an anti-GFP antibody that is particular specific and sensitive for probing yeast-expressed proteins [78].

The approach of using the *GAL*1 promoter was to grow pre-cultures in synthetic medium lacking uracil with 2% glucose, to use an inoculum of this preculture to inoculate synthetic medium lacking uracil with 0.1% glucose, to allow the cells to deplete available glucose, then to add galactose for induction. Although, occurs reduced cell growth following induction, the highest cell density allowed efficient protein expression. Growth on selective "drop-out" media provides selection of cells that retain protein-encoding plasmids [39].

As shown in Figures 6, 7, and 8, expression conditions of the three TAS2Rs under control of *GAL*1 promoter were screened WCF, Immunoblotting and Fluorescence Microscopy following small scale expression from small volumes of cultures. After 22 and 44 hours of incubation of *S. cerevisiae* FGY217 expressing the three TAS2Rs with and in absence of galactose induction, GFP fluorescence was measured by WCF and Western-blot. While WCF measure all fluorescence signal from yeast cells, in Western-blot it is possible to distinguish the GFP-fusion protein (protein of interest) from free-GFP.

Although these differences, the results obtained from WCF and Immunoblotting comparison at 22 hours of induction show identical optimal culture condition for TAS2R39 (induced with 2.5% DMSO at 26°C). However, TAS2R5 and TAS2R7 show different optimal conditions between these two methods. TAS2R5 and TAS2R7 in WCF, both have an optimal culture condition when induced with 2.5% DMSO at 26°C, while in western-bolt increase of expression occurs at 20°C and 26°C, respectively. It is important to refer that, in these experiments, replicas were not performed, so the differences between these two methods might not be significant in the presence of standard deviation. Additionally, cells may emit fluorescence signals in absence of exogenous fluorescent dyes, such as GFP, and this might explain the increase of fluorescence signal over the 44 hours of induction in WCF [77]. For this reason, in this study the optimal culture conditions were selected from Immunoblotting experiments.

Results from Western-blot analysis (Figure 7) show clear bands for each TAS2R-GFP fusion of approximately 41-47 kDa. Although, TAS2R39 exhibited degraded products at lower molecular weights, TAS2R5 and TAS2R7 migrated as a single band in the gel, suggesting that these are stable membrane-integrated receptors [39]. The addition of DMSO (2.5% v/v) with galactose showed to improve TAS2R39 expression. In fact, previous studies reported that the addition of chemical chaperones such as DMSO (2.5% v/v) or histidine (0.04 mg/mL) to yeast cultures increased membrane protein folding [39]. It is known that DMSO is a chemical chaperone that binds and stabilizes the misfolded proteins in the endoplasmic reticulum [39, 46]. Lowering the temperature revealed to improve TAS2R5 expression, resulting from the decrease on the rate of protein synthesis, which might promote the production of properly folded proteins and the integration of those proteins into the membrane [46]. Increase of all three TAS2Rs expression was observed when these receptors are induced with 2%galactose. The *GAL1* promoter induces recombinant heterologous protein expression when galactose is added to the medium. Even though the obtained results are different from the results obtained by Sugawara *et al.* (2009), it is important to refer that in this thesis it was added an additional expression condition (chemical chaperone) which might change some optimal expression culture conditions given by Sugawara and colleagues [46].

Regarding the fluorescence microscopy analysis, it was difficult to determine if TAS2Rs were correctly localized on the cell membrane of *S. cerevisiae*. In the best case scenario, this result might be correlated with the results obtained in WCF, which includes both GFP-fusion and GFP-free into the cell, since it was evident that *S. cerevisiae* FGY217 without any TAS2Rs appear to have free GFP within the cell. This result might be also related to autofluorescence of yeast caused by metabolism products (*e.g.*, glucose) [77]. However, in the worst-case scenario none of the TAS2Rs-GFP fusions are located at the plasma membrane as expected.

Difficulty of lysis is often considered to be a drawback of yeast expression systems. Unfortunately, the cell disruption approach selected, in this case a bead beater, showed an

incompatibility with these TMPs isolation (Appendices – Figure 12 (A, C, and D)). While multiple passes through the homogenizer are required for efficient cell disruption, mechanical and thermal damage to proteins during repeated cycles of shearing can be minimized by conducting a low-speed centrifugation after each pass to separate the disrupted cells in the supernatant from unbroken cells in the pellet so that only the undisrupted cells can be cycled back through the homogenizer [78]. IMAC isolation by histidine tag (His-tag) was also performed (Appendices – Figure 12 (B)), but identical results were obtained leading to two hypotheses: i) problems in the lysis cell method or ii) TAS2Rs are not properly folded and located into the plasma membrane as desired. Consequently, purification of TAS2Rs was not achieved as expression and/or isolation of these transmembrane proteins was difficult to obtain in yeast [39, 78].

Yeast cells contain substantial levels of endogenous protease activity. Deletion of the *PEP*4 gene encoding the Proteinase A of the yeast vacuole has been reported to decrease overall proteolysis because of the role of Pep4p in processing multiple additional pro-forms of proteases in the vacuole. To overcome this problem, it is used a variety of protease inhibitors and the use of a host strain with additional deletion on *PEP*4 gene. In 2011, Clark *et al.*, mentioned that the use of yeast strains with deletions other than *PEP*4 protease-encoding genes also provides significant reductions in proteolytic degradation of purified proteins. Thus, for further studies regarding expression in yeast the implementation of a strain with more protease-encoding genes deletion might be considered [39, 78].

Membrane proteins can be solubilized either from whole-cell lysates or from isolated membrane fractions. It is known that the use of membrane fractions provides higher yield of more readily purified protein. The initial choice of detergents for membrane protein solubilization was based on a previous large-scale analysis that compared the effectiveness of DDM with and without CHS for solubilization of TAS2Rs in *S. cerevisiae* FGY217. In that study, they verified that DDM solubilization efficiency yield increased when combined with CHS, as CHS stabilizes the TAS2Rs. Unfortunately, it was not possible to determine if solubilization of the three TAS2Rs occurred as cell lysis has proven difficult to perform. Consequently, it was not possible to study the interaction between these three bitter taste receptors and polyphenols.

Since cell lysis was difficult to perform, ongoing work is focused on proceeding with BEVS expression system and also evaluate the new signalling system with an engineered *S. cerevisiae* strain to find out if it is possible to study the interaction of TAS2Rs with polyphenols with these systems and overcome the limitations of working with mammalian cells, such high costs for protein production, slow cell growth, expensive media and reagents and culture conditions, such continuous CO_2 supply [43].

5. Conclusion

A set of procedures for expression and purification of transmembrane proteins from the yeast *S. cerevisiae* was described by Drew *et al.* (2008), and these procedures allow cloning of membrane proteins target genes into numerous vectors that provide expression under control of the yeast *GAL*1 promoter resulting in fusion of the targets with different combinations of tags at their C- or N-terminal.

This study allowed to get insights on the best protein expression conditions for these TAS2Rs. Low temperatures and chemical chaperone showed an increase of expression levels. These results suggest that for every receptor the optimal expression time is 22 hours of incubation, but for TAS2R5 the best expression temperature is 20°C, whereas for TAS2R7 it is 26°C and for TAS2R39 it is 26°C combined with 2.5% DMSO. Isolation of TAS2R has been proven difficult due to cell lysis in efficiency and protein degradation.

Nevertheless, functional analysis of purified proteins remains an important part of characterization and definition of conditions suitable for their agonist determination. Although these procedures allow the production of TAS2Rs on a small-scale, there are limitations regarding the expression that may prove difficult to control, such as: 1) Cell density in cultures. It was observed that equal cultures had different cell density when cultured with the same conditions. 2) Efficiency of cell lysis. Although, in few studies, the established procedures on yeast cell lysis were efficient, the fraction of expressed membrane proteins remained in low speed pellet fractions following cell disruption. This might reflect protein in unlysed cells, or is trapped in large organelles at lysis, or even protein that forms large aggregates. 3) Membrane protein solubilization. Therefore, determining an optimum combination of buffer conditions, additives, and detergent might lead to increase in yield. Nevertheless, there remains a possibility that protein fractions which are difficult to solubilize could be denatured or non-native, and for that reason the increased recovery would absolutely be undesirable [39, 78].

The ongoing work is focused on improving the approach to isolate these membrane proteins through yeast overexpression system and, for the same purpose, testing and compare with the baculovirus expression vector system (BEVS). In addition, it is expected to perform TAS2Rs activation by the engineered GPCR-based signalling in yeast, *S. cerevisiae* yWS677, to evaluate polyphenols interaction with these three receptors to understand their relation with bitter taste.

References

[1] Soares, S., Brandão, E., Mateus, N., and De Freitas, V. Sensorial Properties of Red Wine Polyphenols: Astringency and Bitterness. *Critical Reviews in Food Science and Nutrition*. **2015**, 1–45.

[2] Drewnowski, A., and Gomez-Carneros, C. Bitter taste, phytonutrients, and the consumer: a review. *The American Journal of Clinical Nutrition*. **2000**, 72, 1424–1435.

[3] Ashihara, H., and Crozier, A. Caffeine: a well known but little mentioned compound in plant science. *TRENDS in Plant Science*. **2001**, 6, 9, 407–413.

[4] Cleemput, M. V., Cattoor, K., Bosscher, K., Haegeman, G., Keukeleire, D., and Heyerick, A. Hop (*Humulus lupulus*)-Derived Bitter Acids as Multipotent Bioactive Compounds. *Journal of Natural Products*. **2009**, 72, 1220–1230.

[5] Chen, R., Qi, Q.L., Wang, M.T., and Li, Q.Y. Therapeutic potential of naringin: an overview. *Pharmaceutical Biology*. **2016**, 54, 12, 3203–3210.

[6] Salehi, B., Fokou, P. V. T., Sharifi-Rad, M., Zucca, P., Pezzani, R., Martins, N., and Sharifi-Rad, J. The Therapeutic Potential of Naringenin: A Review of Clinical Trials. *Pharmaceuticals*. **2019**, 12 (11), 1–18.

[7] Mazumder, A., Dwivedi, A., and Plessis, J. Sinigrin and Its Therapeutic Benefits. *Molecules*. **2016**, 21, 416, 1–11.

[8] Maehashi, K., and Huang, L. Bitter peptides and bitter taste receptors. *Cellular and Molecular Life Sciences*. **2009**, 66, 1661–1971.

[9] Frank, O., and Hofmann, T. Reinvestigation of the Chemical Structure of Bitter-Tasting Quinizolate and Homoquinizolate and Studies on their Maillard-Type Formation Pathways Using Suitable ^{13}C-Labeling Experiments. *Journal of Agricultural and Food Chemistry*. **2002**, 50, 6027–6036.

[10] Zhang, Y., Lyu, C., Meng, X., Dong, W., Guo, H., Su, C., and Zhang, X. Effect of Storage Condition on Oil Oxidation of Flat-European Hybrid Hazelnut. *Journal of Oleo Science*. **2019**, 1–12.

[11] Xue, A. Y., Pizio, A., Levit, A., Yarnitzky, T., Penn, O., Pupko, T., and Niv, M. Y. Independent Evolution of Strychnine Recognition by Bitter Taste Receptor Subtypes. *Frontiers in Molecular Biosciences*. **2018**, 5, 1–14.

[12] Soares, S., Kohl, S., Thalmann, S., Mateus, N., Meyerhof, W., and De Freitas, V. Different Phenolic Compounds Activate Distinct Human Bitter Taste Receptors. *Journal of Agricultural and Food Chemistry*. **2013**, 61, 1525–1533.

[13] Soares, S., Silva, M. S., García-Estevez, I., Groβmann, P., Brás, N., Brandão, E., Mateus, N., De Freitas, V., Behrens, M., and Meyerhof, W. Human Bitter Taste Receptors Are Activated by Different Classes of Polyphenols. *Journal of Agricultural and Food Chemistry*. **2018**, 66, 8814–8823.

[14] Singla, R. K., Dubey, A. K., Garg, A., Sharma, R. K., Fiorino, M., Ameen, S. M., Haddad, M. A., and Al-Hiary, M. Natural Polyphenols: Chemical Classification, Definition of Classes, subcategories, and Structures. *Journal of AOAC International.* **2019**, 102, 5, 1397 – 1400.

[15] Cardona, F., Andrés-Lacueva, C., Tulipani, S., Tinahones, F. J., and Queipo-Ortuño, M. I. Benefits of polyphenols on gut microbiota and implications in human health. *Journal of Nutritional Biochemistry.* **2013**, 24, 1415–1422.

[16] Freitas, V., and Mateus, N. Protein / Polyphenol Interactions: Past and Present Contributions. Mechanisms of Astringency Perception. *Current Organic Chemistry.* **2012**, 16 (2), 1-23.

[17] Renaud, S., and De Lorgeril, M. Wine, alcohol, platelets, and the French paradox for coronary heart disease. *Epidemiology.* **1992**, 339 (8808), 1523–1526.

[18] Cheynier, V. Phenolic compounds: from plants to foods. *Phytochemistry Reviews.* **2012**, 11, 153–177.

[19] Khoo, H. E., Azlan, A., Tang, S. T., and Lin, S. M. Anthocyanidins and anthocyanins: colored pigments as food, pharmaceutical ingredients, and potential health benefits. *Food & Nutrition Research.* **2017**, 61, 1–21.

[20] Turturicã, M., Oancea, A. M., Râpeanu, G., and Bahrim, G. Anthocyanins: Naturally occurring fruit pigments with functional properties. *The Annals of the University Dunârea de Jos of Galati Fascicle VI – Food Technology.* **2015**, 39 (1), 9–24.

[21] Kuhnle, G. Nutrition epidemiology of flavan-3-ols: The known unknowns. *Molecular Aspects of Medicine.* **2018**, 61, 2–11.

[22] Aron, P. M., and Kennedy, J. A. Flavan-3-ols: Nature, occurrence and biological activity. *Molecular Nutrition & Food Research.* **2008**, 52, 79–104.

[23] Serrano, J., Puupponen-Pimiä, R., Dauer, A., Aura, A.M., and Saura-Calixto, F. Tannins: Current knowledge of food sources, intake, bioavailability and biological effects. *Molecular Nutrition & Food Research.* **2009**, 53, S310–S329.

[24] Aguilar, C. N., Rodríguez, R., Gutiérrez-Sánchez, G., Augur, C., Favelar-Torres, E., Prado-Barragan, L. A., and Ramírez-Coronel, A. and Contreras-Esquivel, J. C. Microbial tannases: advances and prespectives. *Applied Microbiology and Biotechnology.* **2007**, 76, 47–59.

[25] Rue, E. A., Rush, M. D., and Breemen, R. B. Procyanidins: a comprehensive review encompassing structure elucidation via mass spectroscopy. *Phytochemistry.* **2018**, 17 (1), 1–16.

[26] Smeriglio, A., Barreca, D., Bellocco, E., and Trombetta, D. Proanthocyanidins and hydrolysable tannins: occurrence, dietary intake and pharmacological effects. *British Journal of Pharmacology.* **2017**, 174, 1244–1262.

[27] Hoon, M. A., Adler, E., Lindemeier, J., Battey, J- F., Ryba, N. J. P., and Zuker, C. S. Putative Mammalian Taste Receptors: A Class of Taste-Specific GPCRs with Distinct Topographic Selectivity. *Cell.* **1999**, 96, 541-551.

[28] Behren, M., and Meyerhof, W. Bitter taste receptor research comes of age: From characterization to modulation of TAS2Rs. *Seminars in Cell & Developmental Biology.* **2013**, 24, 215-221.

[29] Wiener, A., Shudler, M., Levit, A., and Niv, M. Y. BitterDB: a database of bitter compounds. *Nuclei Acids Research.* **2011**, 40. D413-D419.

[30] Luddi, A., and Governini, L. Taste Receptors: New Players in Sperm Biology. *International Journal of Molecular Sciences.* **2019**, 20, 967 (1-21)

[31] Ueda, T., Ugawa, S., Yamamura, H., Imaizumi, Y., and Shimada, S. Functional Interaction between T2R Taste Receptors and G-Protein α Subunits Expressed in Taste Receptors Cells. *The Journal of Neuroscience.* **2003**, 23(19), 7376-7380.

[32] Yamamoto, K., and Ishimaru, Y. Oral and extra-oral taste perception. *Seminars in Cell & Developmental Biology.* **2013**, 24, 240-246.

[33] Calvo, S., and Egan, J. M. The endocrinology of taste receptors. *Nature Reviews Endocrinology.* **2017**, 11(4), 213-227.

[34] Behrens, M., and Meyerhof, W. Bitter taste receptors and human bitter taste perception. *Cellular and Molecular Life Sciences.* **2006**, 63 (13), 1501-1509.

[35] Dagan-Wiener, A., Pizzio, A., Nissin, I., Bahia, M. S., Dubovski, N., Margulis, E., and Niv, M. Y. BitterDB: taste ligands and receptors database in 2019. *Nucleic Acids Research.* **2019**, 47, D1179-D1185.

[36] Chandrashekar, J., Mueller, K.L., Hoon, M.A., Adler, E., Feng, L., Guo, W., Zuker, C. S., and Ryba, N. J. P. T2Rs Function as Bitter Taste Receptors. *Cell.* **2000**, 100, 703-711.

[37] Peleg, H., Gacon, K., Schlich, P. and Noble, A. C. Bitterness and astringency of flavan-3-ol monomers, dimers and trimers. *Journal of Science of Food and Agriculture.* **1999**, 79, 1123-1128.

[38] Behrens, M., Brockhoff, A., Kuhn, C., Bufe, B., Winnig, M., and Meyerhof, W. The human taste receptor hTAS2R14 responds to a variety of different bitter compounds. *Biochemical and Biophysical Research Communications.* **2004**, *319* (2), 479-485.

[39] Drew, D., Newstead, S., Sonoda, Y., Kim, H., Heijne, G., and Iwata, S. GFP-based optimization scheme for the overexpression and purification of eukaryotic membrane proteins in *Saccharomyces cerevisiae*. *Nature Protocols.* **2008**, 3(5), 784-798.

[40] Freigassner, M., Pichler, H., and Glieder, A. Tuning microbial hosts for membrane protein production. *Microbial Cell Factories.* **2009**, 8 (69), 1-22.

[41] Kollewe, C., and Vilcinskas, A. Production of Recombinant Proteins in Insect Cells. *American Journal of Biochemistry and Biotechnology.* **2013**, 9 (3), 255-271.

[42] Demain, A. L., and Vaishnav, P. Production of recombinant proteins by microbes and higher organisms. *Biotechnology Advances*. **2009**, 27, 297–306.

[43] Aricescu, A. R., Lu, W., and Jones, E. Y. A time- and cost-efficient system for high protein production in mammalian cells. *Acta Crystallographica*. **2006**, D62, 1243–1250.

[44] Rosano, G. L., Morales, E. S., and Ceccarelli, E. A. New tools for recombinant protein production in *Escherichia coli*: A 5-year update. *Protein Science*. **2019**, 28, 1412–1422.

[45] Rosano, G. L., and Ceccarelli, E. A. Recombinant protein expression in *Escherichia coli* : advances and challenges. *Frontiers in Microbiology*. **2014**, 5 (172), 1–17.

[46] Sugawara, T., Ito, K., Shiroishi, M., Tokuda, N., Asada, H., Yurugi-Kobayashi, T., Shimamura, T., Misaka, T., Nomura, N., Murata, T., Abe, K., Iwata, S., and Kobayashi, T. Fluorescence-based optimization of human bitter taste receptor expression in *Saccharomyces cerevisiae*. *Biochemical and Biophysical Research Communications*. **2009**, 382, 704–710.

[47] Sherman, F. An Introduction to the genetics and molecular biology of the yeast Saccharomyces cerevisiae. *The Encyclopedia of Molecular Biology and Molecular Medicine*. **1998**, 302–325.

[48] Sherman, F. Getting started with yeast. *Methods of Enzymology*. **2002**, 350, 3–41.

[49] O'Kennedy, K., and Reid, G. Yeast Nutrient Management in Winemaking. *Australian and New Zealand Grapegrower and Winemaker*. **2008**, 92–100.

[50] Bekatorou, A., Psarianos, C., and Koutinas, A. A. Production of food grade yeasts. *Food Technology and Biotechnology*. **2006**, 44, 407–415.

[51] Carlson, M. Regulation of sugar utilization in Saccharomyces species. *Journal of Bacteriology*. **1987**, 169, 4873–4877.

[52] Held, P. Monitoring growth of beer brewing strains of Saccharomyces cerevisiae. *Application Note*. **2010**, 1–6.

[53] Tissenaum, H. A., and Guarente, L. Model organisms as a guide to mammalian aging. *Development Cell*. **2002**, 1, 9–19.

[54] Alberghina, L., Mavelli, G., Drovandi, G., Palumbo, P., Pessina, S., Tripodi, F., Coccetti, P., and Vanoni, M. Cell growth and cell cycle in *Saccharomyces cerevisiae*: Basic regulatory design and protein–protein interaction network. *Biotechnology Advances*. **2012**, 30, 52–72.

[55] Aucoin, M. G., Mena, J. A., and Kamen, A. A. Bioprocessing of Baculovirus Vectors: A Review. *Current Gene Therapy*. **2010**, 10, 174–186.

[56] Kost, T. A., and Kemp, C. W. Fundamentals of Baculovirus Expression and Applications. *Advances in Experimental Medicine and Biology*. **2016**, 896, 187–197.

[57] Chambers, A. C., Aksular, M., Graves, L. P., Irons, S. L., Possee, R. D., and King, L. A. Overview of the Baculovirus Expression System. *Current Protocols in Protein Science*. **2018**, 91, 5.4.1–5.4.6.

[58] Gupta, K., Tölzer, C., Sari-Ak, D., Fitzgerald, D. J., Schaffitzel, S., and Berger, I. MultiBac: Baculovirus-Mediates Multigene DNA Cargo Delivery in Insect and Mannalian Cells. *Viruses.* **2019**, 11 (3), 1-14.

[59] Hu, Yu-chen. Baculovirus as a highly efficient expression vector in insect and mammalian cells. *Acta Pharmacologica Sinica.* **2005**, 26 (4), 405-416.

[60] Berger, I., and Poterszman, A. Baculovirus expression: old dog, new tricks. *Bioengineered.* **2015**, 6 (6), 316-322.

[61] Berger, I., Fitzgerald, D. J., and Richmond, T. J. Baculovirus expression system for heterologous multiprotein complexes. *Nature Biotechnology.* **2004**, 22 (12), 1583-1587.

[62] Berger, I., and Craig, A. ACEMBL Expression System Series MultiBac^{Turbo} – Multi-Protein Expression in Insect Cells. User Manual, version 3. **2011**, 1-49.

[63] Berger, I., Tölzer, C., and Gupta, K. The MultiBac system: a perspective. *Emerging Topics in Life Sciences.* **2019**, 3, 477-482.

[64] Kost, T. A., Condreay, J. P., and Jarvis, D. L. Baculovirus as versatile vectors for protein expression in insect and mammalian cells. *Nature Biotechnology.* **2005**, 23 (5), 567-575.

[65] Trowitzsch, S., Bieniossek, C., Nie, Y., Garzoni, F., and Berger, I. New baculovirus expression tools for recombinant protein complex production. *Journal of Structural Biology.* **2010**, 2-10.

[66] Scholz, J., and Suppmann, S. A new single-step protocol for rapid baculovirus-driven production in insect cells. *BMC Biotechnology.* **2017**, 17 (83), 1-9.

[67] Johar, S., S., and Talbert, J. N. Strep-tag II fusion technology for the modification and immobilization of lipase B from *Candida antartica* (CALB). *Journal of Genetic Engineering and Biotechnology.* **2017**, 15, 359-367.

[68] Kawate, T., and Gouaux, E. Fluorescence-Detection Size-Exclusion Chromatography for Precrystallization Screening of Integral Membrane Proteins. *Structure.* **2006**, 14 (4), 673-681.

[69] Newstead, S., Kim, H., Heijne, G., Iwata, S., and Drew, D. High-throughput fluorescence-based optimization of eukaryotic membrane protein overexpression and purification in *Saccharomyces cerevisiae*. *Proceedings of the National Academy of Sciences.* **2007**, 104 (35), 13936-13941.

[70] Ley, J. P., Masking Bitter Taste by Molecules. *Chemosensory Perception.* **2008**, 1, 58-77.

[71] Ciancaglini, P., Simão, A. M., Bolean, M., Millán, J. L., Rigos, C. F., Yoneda, J. S., Colhome, M. C., and Stabeli, R. G., Proteoliposomes in nanobiotechnology. *Biophysical Reviews.* **2012**, 4 (1), 67-81.

[72] Gonçalves, R., Mateus, N., Pianet, I., Laguerre, M., and De Freitas, V. Mechanisms of Tannin-Induced Trypsin Inhibition: A Molecular Approach. *Langmuir.* **2011**, 27 (21), 13122-13129.

[73] Venkitakrishnan, R. P., Bernard, O., Max, M., Markley, J. L., and Assadi-Porter, F.M., Use of NMR saturation transfer difference spectroscopy to study ligand binding to membrane proteins. *Methods in Molecular Biology.* **2012**, 914, 47-63.

[74] Sonveaux, N., Vigano, C., Shapiro, A. B., Ling, V., and Ruysschaert, J. M. Ligand-mediated tertiary structure changes of reconstituted P-glycoprotein. A tryptophan fluorescence quenching analysis. *The Journal of Biological Chemistry*. **1999**, 274 (25), 17649-17654.

[75] Shaw, W. M., Yamauchi, H., Mead, J., Gower, Glen-Oliver F., Bell, D. J., Öling, D., Larson, N., Wigglesworth, M., Ladds, G., and Ellis, T. Engineering a Model Cell for Rational Tuning of GPCR Signaling. *Cell*. **2019**, 177, 782-796.

[76] Tkacz, J. S., Cybulska, E. B., and Lampen, J. O. Specific Staining of Wall Mannan in Yeast Cells with Fluorescein-Conjugated Concanavalin A. *Journal of Bacteriology*. **1971**, 105 (1), 1-5.

[77] Maslanka, R., Kwolek-Mirek, M., and Zadrag-Tecza, R. Autofluorescence of yeast *Saccharomyces cerevisisae* cells caused by glucose metabolism products and its methodological implications. *Journal of Microbiology Methods*. 2018, 146, 55-60.

[78] Clark, K. M., Fedoriw, N., Robinson, K., Connelly, S. M., Randles, J., Malkowski, M. G., Titta, G. T., and Dumont, M. E. Purification of Transmembrane Proteins from *Saccharomyces cerevisiae* for X-ray Crystallography. *Protein Expression and Purification*. **2010**, 71 (2), 207-223.

Appendices

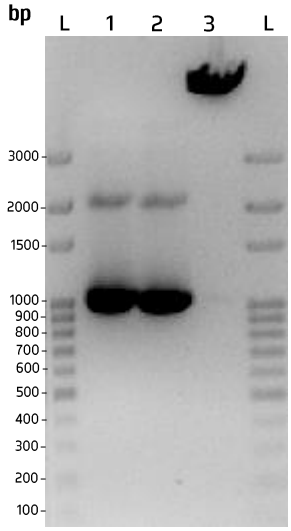

Figure 9. Amplification of TAS2R5_STE2 and linearization of pRS426_GAL1_GFP on agarose gel (0.8%). DNA electrophoresis analysis of the full-length TAS2R5_STE2 amplified by two consecutive PCR's (using primers listed in Table 3). Lanes 1 and 2 are 250x and 100x dilutions from the first TAS2R5_STE2 PCR. An unspecific product was detected at approximately 2200 bp. 1000 bp bands indicate TAS2R5_STE2 DNA sequence. Lane 3 is pRS426_*GAL*1_GFP digest with *Sma*I restriction enzyme.

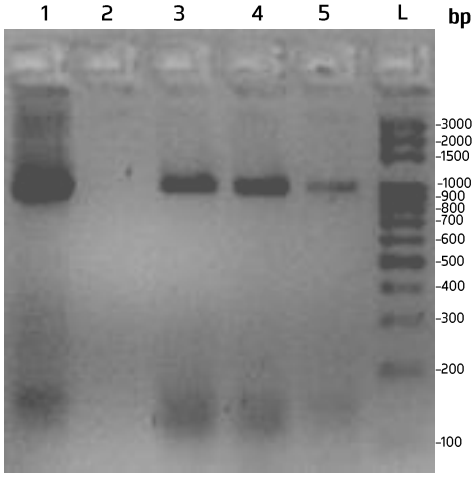

Figure 10. Colony PCR products from *S. cerevisiae* FGY217 on agarose gel (1%) electrophoresis. Amplification was carried out with primers listed on Table 4. PCR results with approximately 900-1000 bp indicate plasmids containing the insert. Lane 1 represents positive control (gel extracted PCR band of TAS2R5_STE2), lane 2 is negative control, lanes 3-5 are colony PCR samples (TAS2R5_STE2_pRS426), and lane 6 is 100 bp ladder (Solis BioDyne).

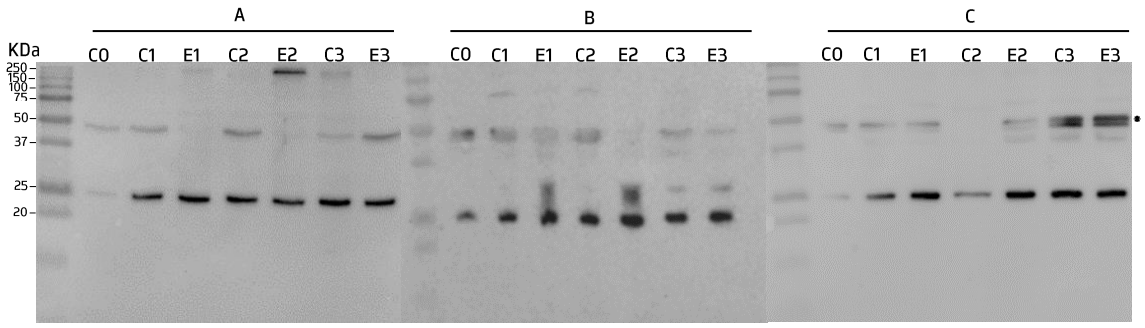

Figure 11. Screening of TAS2R5 (A), TAS2R7 (B) and TAS2R39 (C) expression conditions at 44 hours after galactose induction by Western blotting in *S. cerevisiae* FGY217. Asterisks (*) indicate the bands for TAS2R-GFP fusion proteins, 47 KDa approximately. For each receptor, lane C0 indicates cell suspension before induction; lanes E1, E2, and E3, indicate cell suspension after 22h of induction with 2% galactose under expression conditions; lanes C1, C2, and C3, indicate cell suspensions without induction (0.1% glucose) under expression conditions. C1 and E1 incubated at 26ºC; C2 and E2 incubated at 26ºC with 2.5% DMSO; C3 and E3 incubated at 20ºC (Table 5). Ladder used was Precision Plus Protein™ All Blue Standards (Bio-Rad).

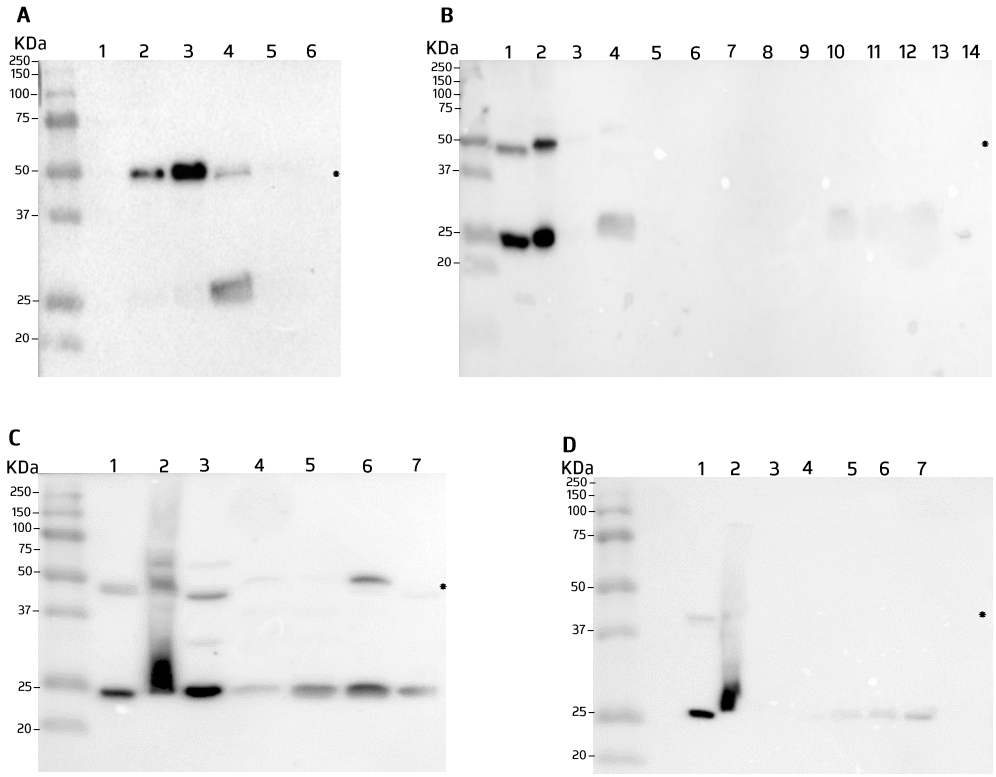

Figure 12. Isolation and solubilization of TAS2R7 by cell membranes fractionation (**A**), His-trap (**B**) and new approach of cell membrane fractionation (**C** and **D**) analysed by Western blotting in *S. cerevisiae* FGY217. Asterisks (*) indicate the bands for TAS2R-GFP fusion proteins, 47 KDa approximately. (**A**) Isolation and solubilization of TAS2R7 by plan A. Lanes 1 and 2 represent the pellet and supernatant after cell lysis, respectively. Lane 3 indicates the supernatant after ultracentrifugation at 120 000 g, for 1h at 4°C. Lane 4 represents the pellet from the last ultracentrifugation resuspended and incubated in buffer B with detergent (1% DDM with 0.2% CHS), for 1h at 4°C. Lanes 5 and 6 indicates supernatant and pellet after ultracentrifugation at 43 000g, for 40 minutes at 4°C, respectively. (**B**) His-Trap approach. Lane 1 represents pellet after 22h of induction under optimal expression condition. Lanes 2 and 3 indicate pellet and supernatant after cell lysis. Lane 4 indicates sample following incubation with detergent (1% DDM with 0.2% CHS) for 4h at 4°C. Lane 5 represents sample after running on His-trap column for 1h45 at 4°C. Lanes 6 and 7 indicate fractions with binding buffer with 10 mM Imidazole. Lanes 8 and 9 indicate fractions with elution buffer with 50 mM Imidazole. Lanes 10 and 11 indicate fractions with elution buffer with 150 mM Imidazole. Lanes 12 and 13 indicate fractions with elution buffer with 300 mM Imidazole. Lane 14 indicate fraction with elution buffer with 500 mM Imidazole. (**C and D**) New approach of cell membrane fractionation. Lane 1 represents pellet after 22h of induction under optimal expression condition. Lane 2 indicates the pellet after cell lysis with the respective fractionation at 2500 g and 4000 g. Lane 3, 4, and 5 represents the pellet and supernatant after centrifugation at 6000 g, respectively, being lane 5 the supernatant 2c more concentrated. Lane 6 represents supernatant after ultracentrifugation at 50 000 rpm, for 1h30 at 4°C. Lane 7 represents the pellet from the last ultracentrifugation resuspended and incubated in buffer B without detergent, for 1h at 4°C.